Analiza mehanike metafaznog diobenog vretena u stanicama HeLa primjenom laserske mikrodisekcije

Polak, Bruno

Master's thesis / Diplomski rad

2015

Degree Grantor / Ustanova koja je dodijelila akademski / stručni stupanj: **University of Zagreb, Faculty of Science / Sveučilište u Zagrebu, Prirodoslovno-matematički fakultet**

Permanent link / Trajna poveznica: https://urn.nsk.hr/urn:nbn:hr:217:998848

Rights / Prava: In copyright / Zaštićeno autorskim pravom.

Download date / Datum preuzimanja: **2024-03-29**

Repository / Repozitorij:

Repository of the Faculty of Science - University of Zagreb

UNIVERSITY OF ZAGREB
FACULTY OF SCIENCE
DEPARTMENT OF BIOLOGY

Bruno Polak

Analysis of metaphase spindle mechanics in HeLa cells by laser microsurgery

Master's thesis

Zagreb, 2015.

This work was done in laboratory of Iva Tolić at Max Planck Institute of Molecular Cell Biology and Genetics, Dresden, under supervision of Iva Tolić. This thesis is submitted for review to Department of Biology at Faculty of Science, University of Zagreb in order to achieve the academic degree Master of molecular biology.

BASIC DOCUMENTATION CARD

University of Zagreb
Faculty of Science
Department of Biology Graduation Thesis

Analysis of metaphase spindle mechanics in HeLa cells by laser microsurgery

Bruno Polak, Rooseveltov trg 6, 10000 Zagreb

Main structure that orchestrates mitosis is the mitotic spindle, and one of the microtubule classes comprised within are the kinetochore fibers, which bind to chromosomes via kinetochores on the centromere. It is currently believed that there is no direct interaction between two sister kinetochore fibers. The focus of this research is to describe a novel class of microtubules in the spindle, which was named bridging microtubules. This new class forms antiparallel bundles, laterally connects sister kinetochore fibers and contributes to spindle mechanics. In conducted research, confocal microscope was used for live-cell imaging of HeLa, and the laser microsurgery was applied on outermost kinetochore fiber in order to confirm bridging microtubule presence and to test their function in force distribution in the spindle. By using cells with decreased level of PRC1 protein, protein involved in metaphase spindle mechanics, we showed that bridging bundle contributes to force balance in the spindle. Microtubule dynamics in the region between sister kinetochores was also analyzed in cells with labeled EB3 protein involved in the growth of microtubule 's + end. Laser microsurgery confirmed compressive and tensile force in the metaphase spindle in both experiments.

(74 pages, 32 figures, 83 references, original in: English)
Key words: mitosis, microtubule, kinetochore, kinetochore fiber, ablation
Supervisor: Dr. sc. Iva Tolić, prof.
Cosupervisor: Dr. sc. Maja Matulić, prof.
Reviewers: Dr. sc. Maja Matulić, prof.
Dr. sc. Mirta Tkalec, izv. prof.
Dr. sc. Duje Lisičić, doc.
Replacement: Dr. sc. Inga Marijanović, doc.
Thesis accepted: June 17 , 2015.

TEMELJNA DOKUMENTACIJSKA KARTICA

Sveučilište u Zagrebu
Prirodoslovno-matematički fakultet
Biološki odsjek Diplomski rad

Analiza mehanike metafaznog diobenog vretena u stanicama HeLa primjenom laserske mikrodisekcije

Bruno Polak, Roosveltov trg 6, Zagreb

Glavna struktura koja upravlja procesom je diobeno vreteno, a jedna od klasa mikrotubula u toj strukturi su kinetohorna vlakna koja vežu kromosome putem kinetohora na centromeri. Trenutne spoznaje govore da dva sestrinska kinetohorna vlakna nisu u međusobnoj izravnoj interakciji. U ovom radu pažnja je usmjerena na opisivanje nove klase mikrotubula u vretenu a nazvana je premošćujući mikrotubuli. Ta nova klasa tvori vlakna antiparalelnih mikrotubula i lateralno povezuje sestrinska kinetohorna vlakna te sudjeluje u mehanici diobenog vretena. U provedenom istraživanju korišten je konfokalni mikroskop za snimanje živih stanica HeLa te je korištena laserska mikrodisekcija vanjskog kinetohornog vlakna, da bi se pokazala prisutnost premošćujućih mikrotubula te ispitala njihova uloga u distribuciji sila u vretenu. Ove su rezultate potvrdili eksperimenti sa stanicama sa smanjenom razinom proteina PRC1 koji je sastavni dio metafaznog vretena. Procesi u regiji između sestrinskih kromosoma analizirani su u stanicama s obilježenim proteinom EB3, uključenim u rast mikrotubula na + kraju. U oba eksperimenta potvrđena je prisutnost kompresivne sile i sile tenzije u metafaznom diobenom vretenu.

(74 stranice, 32 slike, 83 literaturnih navoda, jezik izvornika: engleski)
Ključne riječi: mitoza, mikrotubul, kinetohora, kinetohorno vlakno, ablacija
Voditelj: Dr. sc. Iva Tolić, prof.
Suvoditelj: Dr. sc. Maja Matulić, prof.
Ocjenitelji: Dr. sc. Maja Matulić, prof.
Dr. sc. Mirta Tkalec, izv. prof.
Dr. sc. Duje Lisičić, doc.
Zamjena: Dr. sc. Inga Marijanović, doc.
Rad prihvaćen: 17. lipnja, 2015.

Acknowledgements

First of all, I would like to express my greatest gratitude to my first supervisor, Iva Tolić for giving me a chance to work on this project. For great support, understanding and for the opportunity to become a member of her beautiful Group. Big Thanks to Maja Matulić, my Cosupervisor, for discussions and support.

Biggest thanks go to my family, my brother Robert, mom Vesna, dad Branko, grandma Zdenka and uncle Boris. They are always here for me and I know I can always, always rely on them.

Huge thanks to my godparent Lav and Lidija Kalda for giving me great advice and being super-positive, open-minded and cheerful all the time.

Really amazing thanks go to my best lab mates in the world, Janko Kajtez and Anastasia Solomatina. They taught me everything I know and were amazing during my stay in Germany. Thanks to Emma Stepinac for great team work, discussions, and everything. They were my best friends there and we had the best time in the lab and everywhere.

Undescribeable thanks to all members of Iva Tolić Group in Dresden. Thanks for making me feel welcome and for amazing, precious time in Dresden. Special one goes to Petrina Delivani who was always there for me with understanding, support and approval. Special thanks to Anna Klemm, who was always there for me with great motivation, ideas and advice. Amazing special thanks to Mariola Chacon Rodriguez who was always there as a friend and for trying out different immunocytochemistry protocols. Thanks for going with me for a „cigi“ and saving me and my brother from troubled waters. Huge special thanks to Gheorge and Monica Cojoc who were always super-positive and in a mood for creppes party. Big thanks to Titus Franzman who was always patient enough to teach me something useful and for trusting me with his Western blots (bad idea). Big thanks to Hannes Weisse who made it possible for us to work always. Thanks to Jonas for discussions and for being cool.

Huge thanks to members of Iva Tolić Group in Zagreb. Thanks to Ivana Šarić for understanding, amazing support and for amazing help with Figures. Thanks to Sonja Lesjak for great motivation and support. Thanks to Ana Milas for amazing help with MatLab instructions. Thanks to Kruno Vukušić, Patrik Risteski, Renata Buđa, Ivana Šumanovac Šestak and all the members for being the best Group ever. Big

thanks to Nenad Pavin, Maja Novak, Marcel Prelogović and Matko Glunčić for great discussions. Thanks to Marieta Kralj, Marko Marjanović, Katja Ester and Igor Weber, for a good start with experiments in Zagreb.

Big thanks to Davide Acardi, Sebastian Bundschuh, Jan Peychl and the entire LMF facility for great advice and supervision.

Thanks to Linda Wordeman for providing us with mRFP-CENP-B plasmid, and to Julie Welburn for providing us with 2xGFP-EB3 HeLa cell line. Thanks to FACS facility for making it possible for us to improve our experiments.

Last, but not least, thanks to all my beautiful friends for amazing time we always have together.

Contents

1. Introduction ……..……..1
    1.1. The cell - basics, history and microscopy …….……1
        1.1.2. Cell cycle ……4
        1.1.3. Regulation of mitosis and cell cycle checkpoints ……...7
    1.2. Components of the mitotic spindle ……9
        1.2.1. Centrosomes ……9
        1.2.2. Microtubules ……..10
        1.2.3. Kinetochores ……..12
        1.2.4. Non motor proteins ……14
            1.2.4.1. PRC1 ……..14
            1.2.4.2. End binding proteins ……..15
        1.2.5. Motor proteins ……...16
            1.2.5.1. Kinesins ……..17
            1.2.5.2. Dyneins ……...……18
    1.3. Metaphase spindle - architecture and forces ……...19
    1.4. Spindle assembly and performance ……..22
    1.5. Goal of the research ……..26
2. Materials and methods ……28
    2.1. Cell culture ……...28
    2.2. Imaging and laser microsurgery ……...28
    2.3. RNA interference ……29
        2.3.1. Transfection and sample preparation ……29
        2.3.2. Image analysis ……...30
            2.3.2.1. Velocity of outward movement ……..30
            2.3.2.2. Bridging fiber thickness ……30
            2.3.2.3. Spindle shape ……..31
        2.3.3. Polyacrylamide gel electrophoresis and Western blot ……..31
        2.3.4. Immunocytochemistry ……...32
    2.4. Image analysis in EB3 experiment ……...33
3. Results ……34
    3.1. Set up for microscopy and interpretation of laser microsurgery ……..34

3.2. Self-repair mechanism ……...……...39
3.3. Construction of a cell model for spindle analysis - PRC1 ……41
3.3.1. Analysis of laser ablation in PRC1 - depleted cells ...…….42
3.3.2. Analysis of bridging bundle thickness ……...47
3.3.3. Analysis of the spindle shape ……..49
3.3.4. Analysis of PRC1 expression in siRNA treated cells ……52
3.3.4.1. Immunocytochemistry ……52
3.3.4.2. Western blot ……...53
3.4. Analysis of microtubule dynamics in EB3 experiment ……..……..55
3.4.1. Determination of microtubule growth rate and microtubule dynamics in bridging bundle ……..…56
4. Discussion ……...59
4.1. Force balance in the mitotic spindle ……59
4.2. Junction point ……...62
4.3. Secondary response ……..63
4.4. Dynamics of bridging microtubules ……64
5. Conclusions ……66
6. References ……..……..67
7. Bibliography ……74

1. Introduction

1.1. The cell — basics, history and microscopy

Life is characterized as a system that exchanges energy and substances with its surroundings. It can actively grow, develop and evolve. In addition, it has the ability to react to stimulus and generate new living "offspring". One such living unit is a cell, that can function as a single organism ("one piece puzzle") or as the smallest functional component amongst thousands of other cells, that all together make a multicellular organism as a whole. Whether it lives as a "one piece puzzle" or not, it experiences a series of nano-scale events that are organizing its surface and interior. Eukaryotic cellular components are highly organized to perform the function they are morphologically and structurally specialized for. From cell's membrane through cytoskeleton and organelles, nucleus and genetic material comprised within, there are hundreds of signaling pathways that orchestrate the complex life of a cell. In addition, most cells have the ability to make new ones in a process of duplication of genetic material and eventually, division of the cytoplasm to create two identical daughter cells in a process called mitosis.

To study such a complex system, various methods have been developed, but maybe the most revolutionary one was the idea to magnify it and observe it through a microscope. In 1590's two Dutch spectacle makers, Hans and Zacharias Jansen assembled the first compound microscope by mounting two lenses in a tube. In 1609, Galileo Galilei assembled a compound microscope by combining the convex and concave lenses. Further optical designs and experiments followed as Anton van Leeuwenhoek assembled a microscope with greater magnification, which enabled detailed studies on bacterial cells. In 1931, Ernst Ruska started building the electron microscope and soon after fast progress followed with constructing different types of high resolution microscopes, like a confocal microscope. Even though there were reports on earlier confocal microscopes, the first confocal scanning microscope was built in 1955 by Marvin Minsky and further improvement followed with assembling the confocal laser scanning microscope. This system comprises an optical imaging technique for increasing optical resolution and contrast of a micrograph by means of adding a spatial pinhole placed at the confocal plane of the lens to eliminate out-of-

focus light. Confocal microscope uses point illumination and a pinhole in an optically conjugate plane in front of the detector to eliminate out-of-focus signal - the name "confocal" stems from this configuration. As only light produced by fluorescence very close to the focal plane can be detected, the image's optical resolution, particularly in the sample depth direction, is much better than that of wide-field microscopes [1].

The first person who described the cell as a basic unit of life was Robert Hook, an architect, natural philosopher and scientist. He first used the term in 1665, while looking at thin slices of cork (Figure 1a) [2]. His observations were soon extended to wood and plant tissue, as well as to fly's eye.

The process of duplication and production of new living cells was named mitosis as coined by Walther Flemming. Already in 1880s he drew in detail his observations on mitosis (Figure 1b) [3]. Nevertheless, his study and interpretation of events in the mitosis laid foundations for further research on mitotic cell division.

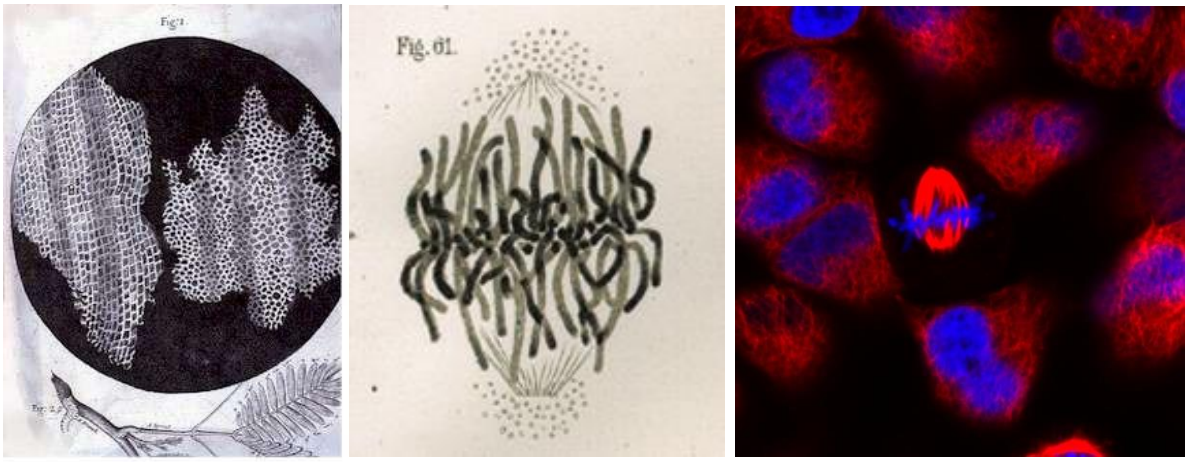


Figure 1. Advances in cell biology: a) Image of a Hook's thin cork sample slice showing cellular organization [2]; b) Flemming's drawing of mitosis with chromosomes and structures today known as components of the mitotic spindle [3]; c) Image of population of HeLa cells stably expressing H2B in mCherry (blue) and tubulin in SiR. Image is acquired with a confocal microscope. In the middle is a HeLa cell in metaphase of mitosis [4].

There are thousands of types of cells comprised within a single multicellular organism, but as there are so many diverse organisms living on planet Earth, this makes a huge variation of cell types one can study. From single cell organisms, neurons, fibroblasts, newt lung cells, to HeLa cells and many more, all of them making a good model system for conducting different types of experiments.

HeLa cells are the oldest used human cell line established by George Gey. They were isolated from a cervical cancer patient Henrietta Lacks and characterized with a previously never seen special feature: immortality- once isolated, they could be kept alive and grow. These cells have been maintained in vitro since their derivation in February, 1951. (Figure 1c) [5].

1.1.2. Cell cycle

The very first living cell must have had a somewhat primitive mechanism of making new ones and some aspects of this process could be evolutionary conserved. The process itself relies on certain complex structures that are newly assembled or disassembled on the onset of mitosis while others are degraded or assembled when mitosis comes to an end. The scenario in which the symmetric distribution of chromosomes in two daughter cells occurs is complex and intriguing. During ~24 hours, cell is going through series of events known as the cell cycle. It is roughly divided in interphase and mitosis (M phase), (Figure 2).

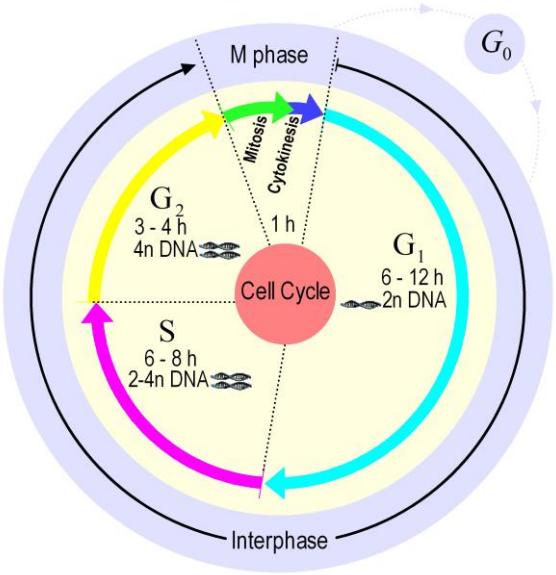


Figure 2. Overview scheme of the cell cycle with pointed G1, S, G2 and M phase. The cell cycle lasts for ~24 hours, with M phase occupying only approximately an hour of the entire cycle [6].

Interphase is a period between two mitotic divisions, during which daughter cell recovers and prepares for the next division. It is divided in G1, S and G2 phase, during which cell doubles its mass of proteins and organelles. “G” in G1 and G2 stands for gap phase and it gives the cell time to feed, grow and to control the accuracy of ongoing events. In S phase that lasts for 10-12 hours, the cell’s genetic material is being duplicated, so that it could be equally distributed to new daughter cells in M phase. During G2 phase certain events are preparing a cells interior for division, as for example duplication of centrosomes. At this point is also possible for cell to enter the, so called G0 phase, which is a resting period that can last for days, weeks or even years before the cell resumes the cell cycle [7]. Mitotic cell division is divided in distinct phases, depending on the organization and behavior of chromosomes. During prophase, which is the beginning of the process, proteins condensins help replicated DNA strands to condense in the nucleus. Thus condensed into structures called chromosomes, the DNA becomes compact and its length is reduced by more than 1000-fold [8]. In the meanwhile, mitotic spindle begins to form between two centrosomes in the cytoplasm. Mitotic spindle is a highly dynamic, complex machinery that orchestrates the progression through mitosis. It is composed of certain structures that direct its behavior, architecture and mechanics. Centrosomes are components that were duplicated in G2 of interphase, and are crucial for establishing the two opposite poles of the spindle. Their duplication also ensures that each daughter cell inherits one. Further on, centrosomes are organizing centers of microtubules, which are highly dynamic structures that make the fundamental part of the spindle. Microtubules are hollow polar structures composed of tubulin subunits. Their minus end is fixed at certain position (e.g. centrosome), while the plus end is more dynamic. In the late prophase, a complex protein assembly is formed on highly condensed DNA on both sides of the centromere. It is called kinetochore, and it is responsible for interaction of chromosomes with the growing microtubules. In pro-metaphase of open mitosis, nuclear envelope breaks down and assembly of mature spindle takes place. This allows the chromosomes to come in contact with microtubules of the mitotic spindle. Alternatively, in closed mitosis typical for yeast cells, nuclear envelope doesn’t breakdown. Once chromosomes become connected to growing microtubules via their kinetochores, active movement of chromosomes can begin. In the next step, during metaphase chromosomes become aligned in the equatorial plane of the mitotic spindle halfway between two poles of the spindle. At

this point sister chromatids are still held tightly bound by multisubunit protein complexes called cohesins. In subsequent anaphase, cohesins are degraded and sister chromatids become separated in a synchronized manner. Once separated in anaphase A, sister chromatids are pulled away from each other towards two poles of the spindle. Kinetochore bound microtubules shorten, and in subsequent anaphase B the distance between two spindle poles increases and chromosomes are effectively pulled further away. As mitosis slowly comes to an end, in telophase separated chromosomes meet the spindle poles and begin to de-condense. At this point, nuclear envelope begins to assemble around each set of chromosomes. On two sides of the former metaphase plate the contractile ring is formed and finally the process comes to completion, when cytoplasm becomes separated by narrowing of the contractile ring (Figure 3) [7]. At this point the nuclear envelopes are fully formed around daughter chromosomes and the production of two identical cells is completed. These newly formed daughter cells can soon begin the same remarkable process.

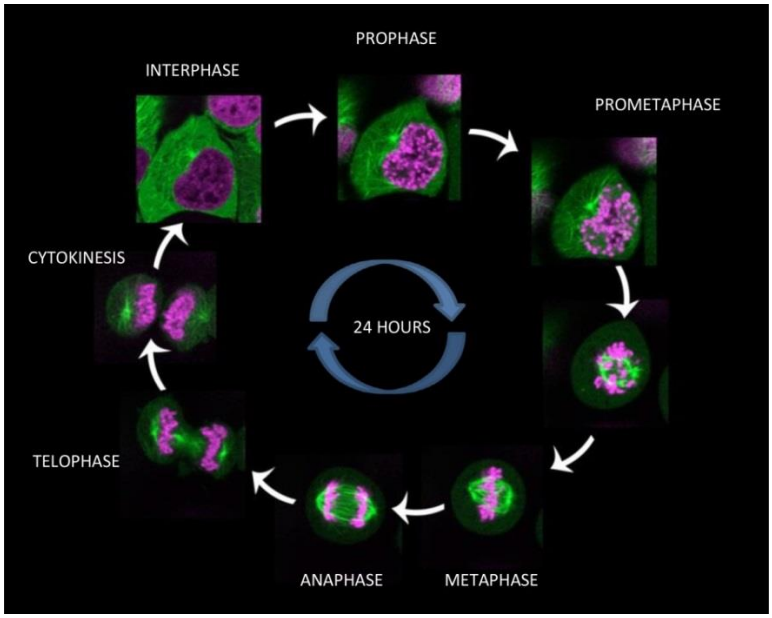


Figure 3. Live images of HeLa cell acquired on a confocal microscope (Zeiss LSM 710 NLO inverted laser scanning microscope, Zeiss, Jena, Germany). This cell line stably expresses tubulin fused to GFP (green) and H2B fused to mCherry (magenta). First image (up left corner) is showing cell in interphase. Following images are summarizing events in mitosis: condensation of chromosomes (prophase); nuclear envelope breakdown and attachment of chromosomes to microtubules of the spindle (prometaphase); alignment of chromosomes in equatorial plane of the spindle (metaphase); segregation of chromosomes (anaphase), narrowing of contractile ring (telophase); division of cytoplasms (cytokinesis).

1.1.3. Regulation of mitosis and cell cycle checkpoints

It is important that the newly formed daughter cells can carry out the same process with as less errors as possible. Since mitosis is a truly fundamental process in continuation of life, the cell has evolved a complex signaling network that regulates and controls a pause or progression through the process itself. Regulation of the cell cycle is evolutionary well preserved amongst all eukaryotic cells. In yeast cells, it has been shown that cdc genes (cell-division-cycle genes) are crucial in passing through the control steps of the cell cycle [9]. The control steps function as a clock, which can stop so as to give time for an appropriate machinery to be fixed or to fix the encountered error. Basically, this system delays certain sequential steps of the cycle, if necessary, and is regulated by means of negative intracellular signals. At the heart of the cell cycle control system is a family of protein kinases known as cyclin-dependent kinases (Cdks), which are present in a cell in constant levels but are cyclically active. By phosphorylating certain intracellular proteins, they regulate DNA replication, mitosis and cytokinesis- major events in the cell cycle [7]. Cdks are regulated by cyclins, which can bind to cdks and activate them. Since the cyclins themselves undergo cyclic synthesis and degradation, cdks' activity depends on the abundance of cyclins in the cell. There are 3 described checkpoints that control the accuracy of fundamental events (Figure 4). In G1 checkpoint, also known as the restriction checkpoint, a control mechanism ensures that the conditions are favorable for cell to enter the S phase. Since G1 is the first phase after cytokinesis, this control step checks "how the cell is feeling", and when is the right time to continue the cycle. If conditions are favorable, a cell can proceed past restriction point and begin the duplication of DNA, or it can, alternatively, enter the G0 quiescent state, thus postponing S phase. During G2 checkpoint, just finished DNA synthesis is checked for damage and errors that could have occurred during DNA replication. At this point a cell can either enter mitotic division or delay it. The final checkpoint, called the spindle checkpoint, occurs in metaphase to ensure that chromosomes are properly attached to microtubules of the mitotic spindle and aligned in the metaphase plate [10]. This checkpoint is the last barrier for chromosomes to get separated in the following anaphase. Described checkpoints control the progression through the cycle and the cell relies on these mechanisms to ensure correct DNA replication and

chromosome segregation, proper division of cytoplasm and finally production of two healthy, functional daughter cells.

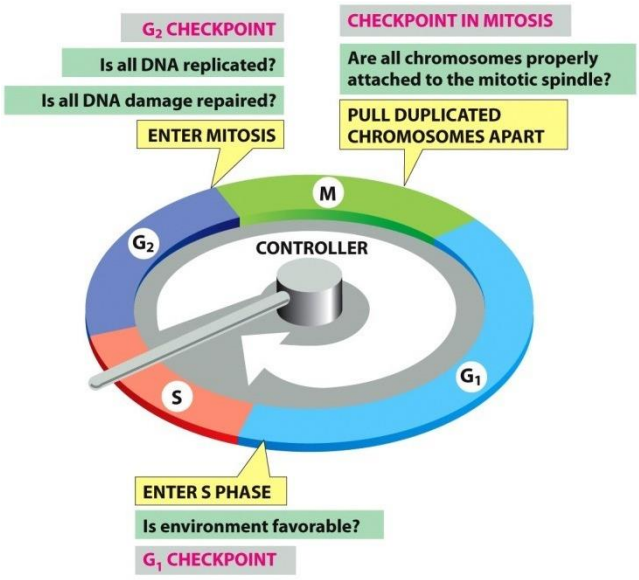


Figure 4. Scheme of a cell cycle with timing of restriction points. G1 checkpoint makes sure that the conditions are appropriate for DNA duplication. G2 checkpoint checks whether DNA was duplicated without errors. Mitotic spindle checkpoint (checkpoint in mitosis) ensures that all chromosomes are properly attached to k-fibers and oriented in a way that they could be pulled to centers of new daughter cells [11].

1.2. Components of the mitotic spindle

During mitosis recruitment of different proteins is crucial. Many of them build up the structures that orchestrate the mitosis itself. One such macromolecular structure is the mitotic spindle that pulls duplicated chromosomes apart.

1.2.1. Centrosomes

Centrosomes are microtubule organizing centers (MTOC) in animal cells. They are composed of two centrioles and associated pericentriolar matrix (Figure 5). Centrosomes and associated components determine the geometry of microtubules arrays throughout the cell cycle, and thus influence cell shape, polarity and motility, as well as spindle formation, chromosome segregation and cell division [12]. All centrosomes contain a structured core to which more than 50 copies of γ-tubulin ring complex (γ-TuRC) are connected [8]. Each γ-TuRC contains 13 copies of γ-isoform of tubulin that define the position of microtubule nucleation, the polar orientation of the polymer, and the lattice into which tubulin assembles [13]. Although they are involved in many events throughout the cell cycle, their possibility to form two poles of the spindle and to nucleate microtubules makes them an important component of the spindle. Centrosomes are duplicated in interphase in a process known as the centrosome cycle. Once duplicated, centrosomes move to opposite sides of the nucleus where they form two poles of the future spindle. As the nuclear envelope breaks down in pro-metaphase, they nucleate microtubule asters that will build up the mitotic spindle.

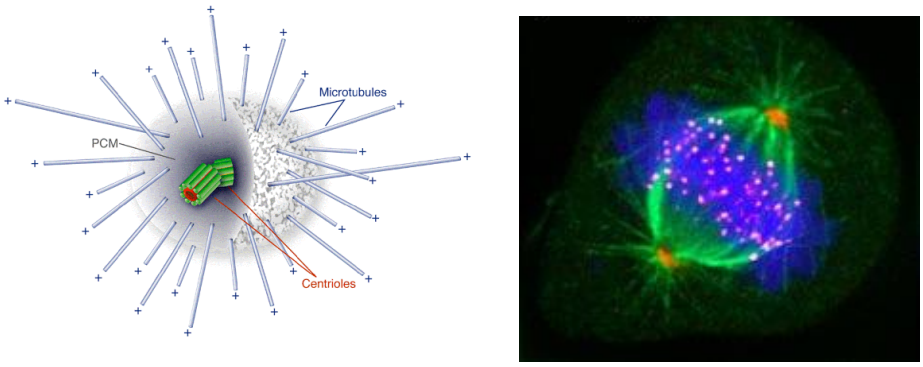


Figure 5. a) Scheme of a centrosome with major components pointed out: centrioles as the central structure, pericentriolar matrix and nucleated microtubules [14]. b) Image of mitotic cell with centrosomes labeled red, microtubules green and kinetochores magenta. Centrosomes in red represent two poles of the spindle [15].

1.2.2. Microtubules

Microtubules are a cytoskeletal component of the cell, composed of protein tubulin. The tubulin subunit is a heterodimer formed from two closely related globular proteins α and β tubulin, tightly bound together by non-covalent bonds. Microtubules are assembled as long, hollow cylinders with an outer diameter of 25 nm. This cylindrical structure is built from 13 protofilaments, each composed of alternating α-tubulin and β-tubulin molecules [7]. Both α and β monomer can bind one molecule of GTP. If it is bound to α tubulin, GTP will never be exchanged or hydrolyzed, while β-tubulin bound GTP can undergo hydrolysis to produce GDP. This hydrolysis has an important effect on microtubule dynamics. Indeed, microtubules often switch between phases of growth and shrinkage. This remarkable behavior was discovered in 1984 when Tim Mitchison and Marc Kirschner [16] deduced that microtubules switch from growth to shrinkage when they lose their GTP caps: "We report here that microtubules in vitro coexist in growing and shrinking populations which interconvert rather infrequently. The dynamic instability is a general property of microtubules and

may be fundamental in explaining cellular microtubule organization". Today we know that they possess intrinsic polarity with their minus ends embedded in MTOC, e.g. centrosome, while the (free) plus end is more dynamic and switches fast between growth and shrinkage, a.k.a. catastrophe (Figure 6). Microtubules grow when αβ-tubulin collides with the end of a protofilament and forms a non-covalent bond. These collisions occur more frequently when the tubulin concentration is higher, and thus the growth rate increases linearly with more tubulin [17]. Microtubule ends with bound GTP are stable and polymerize, whereas ends containing GDP are unstable and depolymerize. In addition, there is a possibility for microtubules to switch from shrinkage to growth in a process known as rescue. Driving these processes are a host of microtubule-associated proteins (MAPs) that make microtubules grow faster, shrink slower, undergo catastrophe more often, and so on [18]. This, so called, dynamic instability is particularly frequent within microtubule populations that build up the mitotic spindle. Microtubules of the mitotic spindle are more dynamic than ones present in interphase, with complete exchange of spindle microtubules and soluble subunits occurring within seconds [19]. Already in 1950s Shinya Inoué [20] observed that spindles are made of aligned protein fibers that exist in rapid dynamic equilibrium with a pool of unassembled subunits. He proposed that spindle fiber disassembly generates force to move chromosomes. Indeed, once the nuclear envelope breaks down in pro-metaphase, chromosomes become free to make contact with the growing microtubules via their kinetochores. These, kinetochore bound, microtubules are called k-fibers and they generate forces on chromosomes throughout mitosis. During prophase, these forces direct the alignment of chromosomes to the metaphase plate and in anaphase they are directed to segregate chromosomes and pull them towards each pole of the spindle.

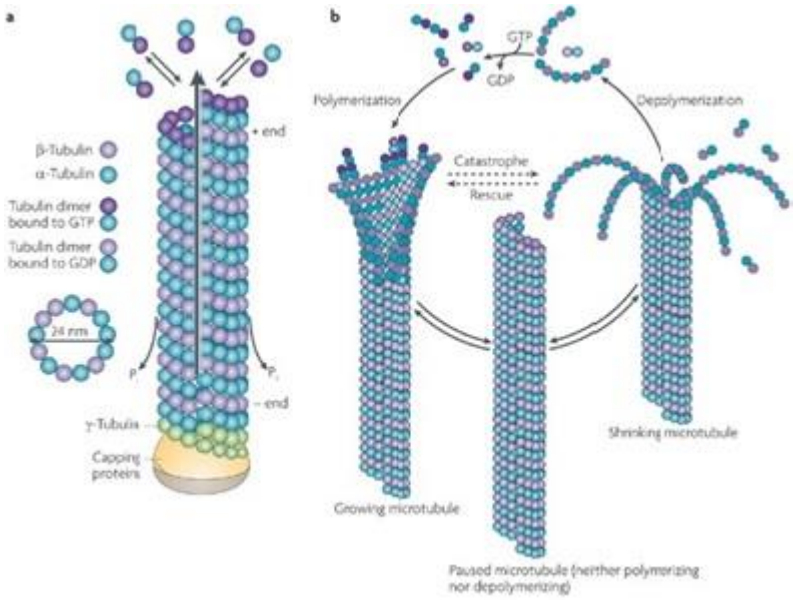


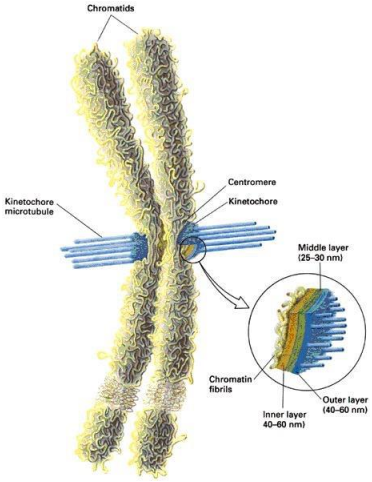
Figure 6. Scheme of microtubules with depicted growth and shrinkage as their dynamic property [21].

1.2.3. Kinetochores

Kinetochores are large, sticky protein complexes formed on centromeric regions of chromosomes during late prophase. For high-fidelity chromosome segregation, kinetochores must be correctly captured by microtubules of the mitotic spindle before anaphase onset. The vertebrate kinetochore, as seen by transmission electron microscopy, appears as a trilaminar stack of plates that is situated on opposite sides of the centromeric heterochromatin of the mitotic chromosome [22]. The properly assembled kinetochore contains two main regions (Figure 7). The inner one is tightly associated with the centromeric DNA and appears like a discrete heterochromatin domain throughout the cell cycle. The outer, highly dynamic plate is the site of interaction with the growing microtubules. In vertebrate cells, it contains about 20 anchoring sites for plus ends of growing microtubules of the spindle. Additionally, it has been shown that kinetochores can nucleate microtubules, both on isolated mitotic human chromosomes [23] as well as in vivo [24; 25]). These kinetochore-nucleated microtubules may speed up kinetochore capture and the process of spindle assembly

[26; 27]. During pro-metaphase, microtubules nucleated at centrosomes grow and shrink rapidly until they encounter and bind to kinetochore by pivoting of microtubules around the centrosome [28]. Once this connection occurs on both sister kinetochores (on two sides of centromeric region), which links chromosome to opposite spindle poles, the bipolar orientation of a chromosome is established. Thus formed orientation is crucial for establishment of forces that will act on chromosomes throughout the following events in mitosis.

a)



b)

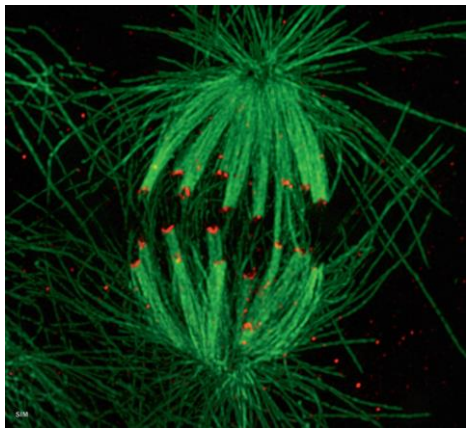


Figure 7. a) Scheme of a chromosome with two chromatids as seen in M phase of the cell cycle. Kinetochore is positioned in a centromeric region of each chromatid with inner layer connected to chromatin fibrils, outer layer that both nucleates and binds microtubules, and middle layer in between [29]. b) Image of mitotic cell with kinetochores labeled red and microtubules green. Dense green signal corresponds to k-fibers bound to kinetochores [30].

1.2.4. Non motor proteins

In addition to fundamental microtubules and described components, a crucial role has to be assigned to microtubule associated proteins (MAPS) and motor proteins. These proteins direct the assembly, behavior and performance of the spindle. MAPs act as structural elements of the microtubule component of the cytoskeleton and mitotic spindle. Some MAPs stabilize the assembled polymer, whereas others mediate the interaction between individual microtubules and between microtubules and other components of the cytoskeleton. Non-motor proteins promote the formation and maintenance of mitotic spindles through diverse mechanisms including the nucleation and organization of microtubules, influence on motor function, and regulation of cell cycle control. In general, these proteins are relatively large, and many are only expressed during G2/M phase of the cell cycle [31]. They can act as cross-linkers that hold microtubules in close vicinity. For example, NuMa binds microtubules directly and mechanically crosslinks microtubules at spindle poles [32]. Some non-motor cross-linking proteins mutually stabilize antiparallel microtubules in the spindle mid-zone. Others act as end binding proteins that control microtubule dynamics and persistent microtubule growth. Further on, non-motor proteins can interact with motor proteins. In some circumstances, the interaction is direct and the non-motor protein controls the function of the motor protein [32].

1.2.4.1. PRC1

Protein regulator of cytokinesis 1 (PRC1) is a midzone-associated protein required for cytokinesis and its bundling activity is crucial for the formation of spindle's midzone. Its C-terminal domain binds to microtubules and N-terminal domain is necessary for dimerization. The rod domain located in between, together with the N-terminus facilitates binding of other proteins, for example kinesin-4. Its microtubule bundling is regulated by Cdk phosphorylation in a way that, when phosphorylated, it can bind to microtubules but cannot cross-link them. Once dephosphorylated, it can cross-link microtubules and form antiparallel bundles. PRC1 works in tandem with kinesin-4 which translocates it to the midzone in metaphase [33].

1.2.4.2. End binding proteins

Growing microtubules accumulate at their plus ends multiple structurally unrelated factors collectively termed MT plus-end tracking proteins, or +TIPs. The most conserved and ubiquitous +TIPs are end binding proteins (EBs) [34]. They are core components of microtubule plus-end tracking protein networks. EBs are relatively small dimeric proteins which contain an N-terminal calponin homology (CH) domain, responsible for the interaction with microtubules, a linker region of unknown function, and a C-terminal coiled coil domain that extends into a four-helix bundle, required for dimer formation [35]. Through their C-terminal sequences, EBs interact with most other known +TIPs and recruit many of them to the growing microtubules ends [36]. Structural studies suggest that the EBs probably act by enhancing lateral interactions between individual protofilaments and may affect MT lattice structure [37; 38]. Mammalian cells express three members of the EB family- EB1, EB2 and EB3. It has been shown in mouse fibroblasts that EB1 is involved in formation of stable microtubules and that simultaneous depletion of EB1 and EB3 increases microtubule catastrophe frequency and disrupts persistent microtubule growth [35]. EB3 localizes throughout the cell cycle only to the plus ends of growing microtubules [39], and accumulates at the centrosome [40; 41; 42], from early prophase until the end of mitosis, concurrently with the increase of microtubule nucleation rates at the centrosome [43]. In mitosis, microtubule property to switch between growth and catastrophe becomes important for generating forces on chromosomes. This dynamic instability is, not exclusively, but still highly regulated by exchange of EBs and GTP/GDP.

1.2.5. Motor proteins

Motor proteins move across cytoskeleton and actively organize cell's interior. By using energy, they make traffic of all intracellular components possible. Transport inside the cell requires forces to move and position various molecular assemblies and organelles. These forces are mostly generated by motor proteins such as myosin, kinesin and dynein. To exert forces, motor proteins bind with one end to cytoskeletal filaments and with the other end to the cell cortex, a vesicle or another motor [44]. Whilst myosins are associated with contractile activity in muscle and non-muscle cells, kinesins and dyneins are microtubule motor proteins. Cytoskeletal motor proteins use structural changes in their nucleoside-triphosphate-binding sites to produce cyclic interactions with a partner protein. Further on, each cycle of binding and release must propel them forward in a single direction along a filament to a new binding site on the same filament. For such unidirectional motion, a motor protein must use the energy derived from ATP binding and hydrolysis to force a large movement in part of the protein molecule (Figure 8), [7]. The organization of microtubules into the highly ordered bipolar array of the mitotic spindle depends on activities of numerous motor and non-motor microtubule-associated proteins. Motor proteins have received significant attention because they generate force on microtubules during spindle formation and throughout mitosis. In that way, motor proteins actively walk across microtubule fibers and direct their active movement, thus, for example, controlling the separation of mitotic spindle poles. Some of the motor proteins form oligomers that can crosslink adjacent microtubules, and in that way they can move one microtubule relative to the other, with the direction of movement dependent on the polarity of both motor protein and microtubules. Alternatively, such motor proteins can slide antiparallel microtubules past each other in the overlap zone of the spindle.

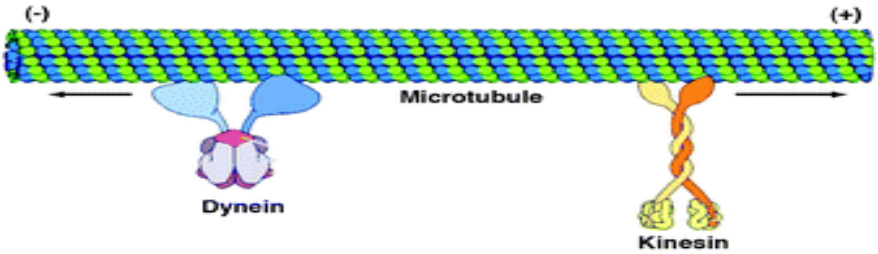


Figure 8. Scheme of direction of the motor proteins moving along a microtubule. Note that some proteins in kinesin family have the ability to move towards minus ends as well [45].

1.2.5.1. Kinesins

There are approximately 14 families of kinesin-related proteins (KRPs). Most of them walk towards plus end of the microtubule, but in addition to this behavior, some walk towards the minus end, and some depolymerize microtubules. At the cellular level, kinesin motors perform a variety of functions during cell division and within the mitotic spindle where they help chromosomes get segregated with the highest fidelity possible [46]. Their structure can roughly be summarized in having two heavy chains and two light chains per active motor, two globular head motor domains, and an elongated coiled-coil responsible for heavy chain dimerization. Most kinesins have a binding site in the tail for either a membrane organelle or another microtubule, thus giving them specific roles in mitotic and meiotic spindle formation and chromosome separation during cell division. The fastest kinesins can move their microtubules at about 2-3 μm/sec [7].

1.2.5.2. Dyneins

The dyneins are a family of minus-end-directed microtubule motors and are unrelated to kinesin superfamily. They are composed of two or three heavy chains, including motor domain, and a large and variable number of associated light chains. The dynein family has two major branches. Cytoplasmic dyneins are found in, probably all eukaryotic cells. They have a role in vesicle trafficking and in localization of the Golgi apparatus near the center of the cell. Other branch contains the axonemal dyneins which are highly specialized for the rapid and efficient sliding movements of microtubules that drive the beating of cilia and flagella, as well as of one's orchestrating mitosis. Dyneins are the largest of the known molecular motors, and they are also among the fastest with the ability to move their microtubules at the remarkable rate of 14 μm/sec [7].

1.3. Metaphase spindle – architecture and forces

There are many crucial points in mitosis, but maybe the most important one is the capture of chromosomes by microtubules of mitotic spindle. Spindle microtubule minus ends are focused into two poles which dictate where segregated chromosomes are transported at anaphase. Forces that focus microtubules into poles are crucial to spindle organization and function. In order to maintain its structural integrity, it is crucial for the spindle to be able to continuously rebuild poles by reorganizing and sorting new microtubule structures [47]. Once in contact with the spindle apparatus, chromosomes slowly become aligned in the metaphase plate and are at this point waiting to be pulled apart.

Different classes of microtubules that are all assembled from the same pool of tubulin subunits contribute to spindle's shape and architecture. They are all extremely dynamic and are generally organized with their minus ends at or near the spindle poles and with their plus ends extending outward to from three distinct populations that make the spindle [48]. Astrals grow in all directions and interact with cell cortex, while inter-polar microtubules and k-fibers grow towards mid-zone (Figure 9).

Microtubules that bind to kinetochores with their plus ends, become k-fibers that can exert a pushing or a pulling force on chromosomes. It has been shown in high resolution electron microscopy tomography that there are two distinct fibrous connections between the kinetochore and k-fiber microtubules. One set of fibers directly encircles the tip of the microtubule and another set of fibers attach to the microtubule wall. Since the organization of the outer plate of the kinetochore resembles a spider's web, it is possible for the kinetochore to interact with microtubules at various angles [49]. In that way, one chromosome with two chromatids and two sister kinetochores gets connected to opposite spindle poles via two sister k-fibers. Thus formed bi-orientation of chromosomes on the mitotic spindle makes it possible for microtubules to exert certain forces on kinetochores, which are partially driven by microtubule's dynamic instability. Some of these forces act on chromosomes but most are generated at the kinetochore, and they don't seem to depend on the number of microtubules in a k-fiber [49]. Once these forces get established they are directed to move chromosomes back and forth until they become aligned in the spindle midzone, i.e. equatorial plate or metaphase plate. Once established, metaphase, from physical point of view, becomes a stable state as all

forces acting within the spindle are accurately balanced and parameters describing the system reach and hold stationary values [50]. At this point spindle's steady-state length is determined through the integrated action of mechanisms that generate and respond to mechanical forces [51]. The axis connecting two spindle poles defines the spindle length, whilst the axis connecting two opposite outermost sister kinetochore pair is considered as spindle width. In addition to basic components of the spindle, motor and nonmotor proteins also play a significant role in establishing spindle length. In particular, the balance between plus-end-directed and minus-end-directed motor proteins can determine spindle length. Increasing the level of one of the plus-end-directed motor proteins produces abnormally long spindles, whilst increasing the level of one of the minus-end-directed motor produces abnormally short spindles. This balance between opposing motor proteins is regulated by certain Cdks (M-Cdk) in a way that at least one of the motor proteins has to be phosphorylated in order to bind to the spindle [7]. The length of the spindle is maintained by overlapping antiparallel microtubules that are pushed outward by molecular motors. In this way the inward tension in the microtubules connecting the poles with kinetochores is balanced. Additionally, it is expected for the spindle length to depend on cell size, since the function of this assembly is to physically move sister chromatids into the center of nascent daughter cells. Length is important for spindle function and it typically increases with cell size and genome size [52]. It has been shown that spindle length increases with cell length in small cells, but in very large cells spindle length approaches an upper limit [53]. Once established, spindle length can have certain effects on spindle performance and segregation of chromosomes.

In addition to k-fibers, non-kinetochore microtubules comprise the majority of microtubules in mammalian spindles that have been studied by electron microscopy. During metaphase, they bundle together 30-50 nm apart in groups of 2-6, with anti-parallel interactions apparently preferred [54]. Their function is poorly understood, but it is believed that they help integrate the whole spindle and ensure its bipolarity. Contrary to many textbook models, their minus ends are not simply located at poles, but rather throughout the spindle [55]. Although antiparallel microtubules are a bit of a mystery, it is known that they form overlapping bundles in the spindle midzone. It is the place to which many motor and nonmotor proteins get recruited. For example kinesin-14 and kinesin-5 are capable of sliding antiparallel spindle microtubules. Kinesin-14 is a minus end directed motor and it is believed to promote spindle

shortening (inward directed force), whilst kinesin-5 probably promotes increased spindle length (outward directed force) [56].

Astral microtubules grow in all directions whilst having their minus ends fixed at centrosome. Whilst growing, some eventually encounter cell cortex and establish certain interactions that could have a role in positioning the spindle within the cell. They turnover at a rate similar to non-kinetochore microtubules [57] and are capped by gamma-tubulin complexes at centrosomes. In contrary to antiparallel microtubules, these do not appear to slide [58].

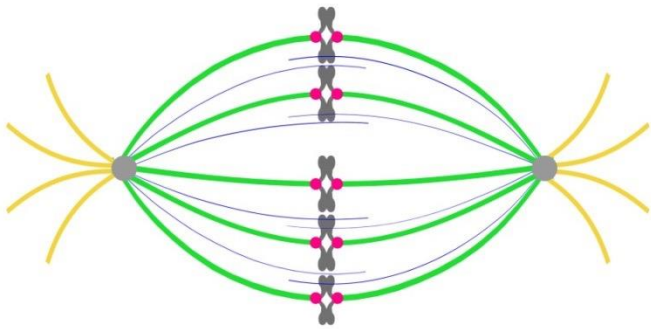


Figure 9. Scheme of the mitotic spindle with different populations of microtubules present within. Astrals, shown in yellow, grow in all directions. K-fibers, shown in green bind to kinetochores on chromosomes. Antiparallel microtubules, shown in thin blue lines, are mutually cross-linked in the spindle midzone.

1.4. Spindle assembly and performance

Mitotic spindle begins to form in prophase between two centrosomes that were previously duplicated in interphase. The initial stages of spindle assembly are marked by motor-dependent separation and movement of centrosomes to opposite sides of the prophase nucleus [56]. Thus separated, they will form two poles of the spindle. Cytoplasmic dynein clusters parallel microtubules into spindle poles [59] and transports NuMa to build poles [32]. At poles, dynein and NuMa tether microtubules in a way that pole structure remains robust despite dynamic instability of microtubules [60].

Centrosomes nucleate microtubules of the spindle. Most of them will search for kinetochores, but only ones that grow towards spindle midzone can encounter and capture them. Microtubules extend from centrosomes preferentially in the direction of chromosomes which is dependent on concentration gradients of RanGTP and its associated proteins around chromosomes [28]. Ran is a member of GTPase family, and it facilitates microtubule rescue, bi-polar spindle formation, and kinetochore-microtubule interactions. First requirement for growing microtubules to start searching at all is that the nuclear envelope breaks down, which happens in pro-metaphase. After this event, chromosomes become free to get caught by the growing microtubules. As a microtubule grows from the centrosome in an arbitrary direction, it probes the space as it searches for kinetochores. Even though a single microtubule probes only one direction, numerous directions will be explored eventually because numerous microtubules grow from the centrosome [28]. Once kinetochore is encountered, its proper capture is achieved in a stepwise manner. First, kinetochores are captured by the lateral surface of a single microtubule that extends from either spindle pole. Once captured, kinetochore is transported poleward along the microtubule [61], until the end-on connection is established (Figure 10). After the initial microtubule capture, kinetochores develop a bundle of 15-30 parallel microtubules that connect them to spindle poles. In a mature k-fiber, tubulin heterodimers are constantly added in the kinetochore and removed from the minus ends in the pole thus promoting k-fragment elongation [27].

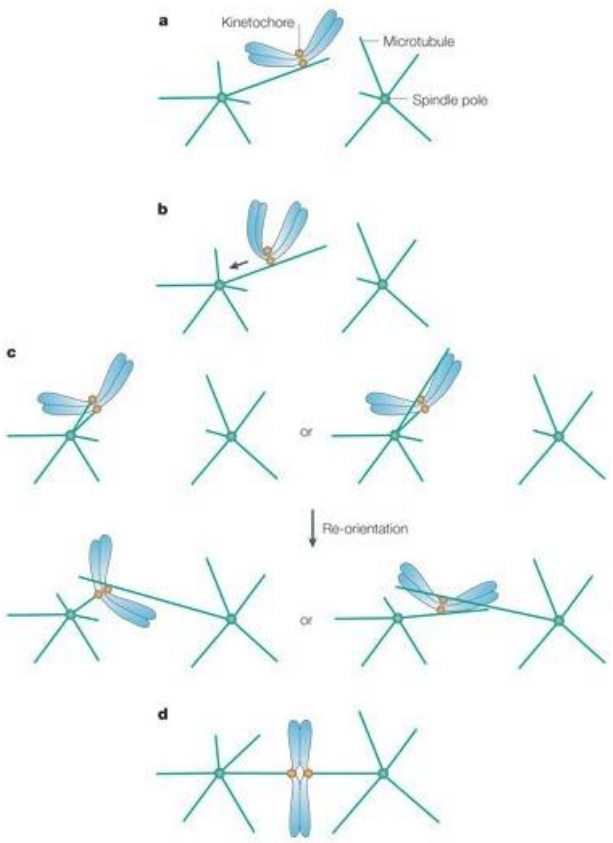


Figure 10. Scheme of kinetochore attachment and establishment of biorientation. a) Kinetochore captured by a lateral surface of a growing microtubule that extends from one pole. b) After first established interaction, kinetochore is transported towards the pole from which the microtubule it is bound to originates. c) Certain events at this point are not clear but at this point a certain mechanism will ensure that kinetochores eventually become properly bioriented. d) Kinetochores become properly bioriented when they are attached to microtubules extending from opposite poles [61].

In addition to, so called, centrosomal pathway that nucleates microtubules of the spindle, there is also a chromatin mediated pathway. In cells lacking centrosomes, spindle can be assembled through chromosome directed pathway. In fact, those cells rely exclusively on this pathway in which microtubules are nucleated and stabilized near chromosomes and kinetochores by the RanGTPase [62] and the chromosomal passenger complex (CPC) [63]. CPC complex is a combination of various proteins that all combined help the assembly and maintenance of the spindle. Dasra A and

Dasra B have been identified as components of the CPC containing Incenp (inner centromere protein), Survivin, (member of the inhibitor of apoptosis family) and the kinase Aurora B. Aurora B has the role in attachment of the mitotic spindle to the centromere as it localizes to k-fiber region near kinetochores. This complex targets to different locations at different times during mitosis, where it regulates correction of microtubule attachment errors, activates spindle assembly checkpoint and regulates contractile apparatus that drives cytokinesis [64].

Once all chromosomes become bi-oriented, they begin to oscillate in the spindle midzone. Both microtubule attachments and dynamics at the kinetochore contribute to sister kinetochore oscillation. Plus and minus end-directed motors associate with kinetochores, suggesting that motors could drive the movement of chromosomes either towards or away from the spindle equator [65]. The velocity of chromosome movement is rather constant, occurring at 2 μm/min, which is consistent with the rates of motor proteins associated with kinetochores [66]. For example, microtubule depolymerizing kinesin MCAK is important for sister kinetochore coordination during oscillations [67]. Eventually, chromosomes actively get positioned in the equatorial plane of the spindle in metaphase. Congression of the last chromosome marks the transition to the metaphase, during which oscillations are continued until cohesins are broken down and at this point chromosomes are readily segregated.

It has been proposed that the synchrony of chromatid-to-pole movement during anaphase A depends on the poleward flux of spindle microtubules. Poleward microtubule flux occurs due to the depolymerization of microtubule minus-ends and is driven mostly by members of the kinesin-5 family of motors which push microtubule minus-ends apart. This movement pulls kinetochores apart thus helping chromosomes segregate. It is also thought that anaphase A movement is driven by depolymerization of k-fibers at the kinetochore.

Poleward flux drives spindle elongation in anaphase B. Kinesin-5 motor was proposed to drive antiparallel microtubules slide apart thus exerting force on the spindle poles. At the same time, depolymerization of the minus ends at poles is stopped, poleward flux is turned off and interpolar microtubules exert pushing force on the spindle poles thus separating spindle poles with approaching chromosomes.

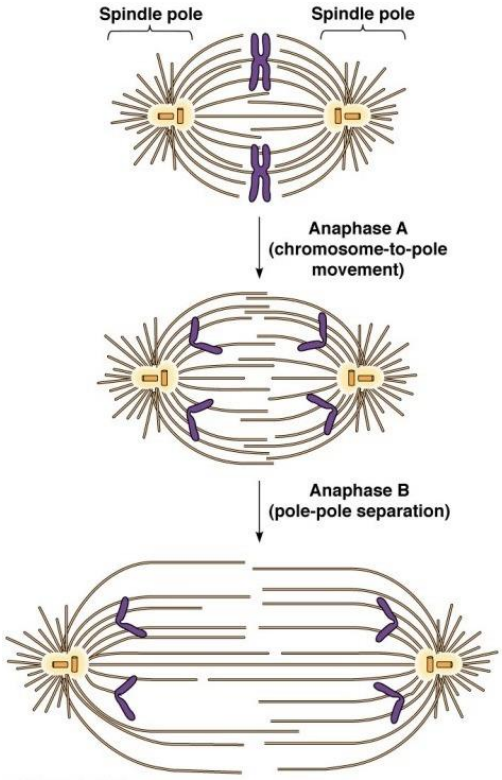


Figure 11. Scheme of anaphase A and B mechanism. First, in anaphase A separated chromosomes are pulled towards opposite poles. Soon after, in anaphase B poles move more apart pulling the attached chromosomes to the center of two new daughter cells [68].

1.5. Goal of the research

The goal of this research is to study nature of the mitotic spindle in HeLa cells, to understand its mechanics and to refresh currently known facts about architecture of the spindle as a whole. Due to spindles appearance and structural complexity, it is difficult to understand its components whilst it is intact and unperturbed. For this reason, laser microsurgery was applied. Behavior of the ablated part of the spindle makes it possible to analyze the distribution of forces acting within it. Additionally, the response to the cut shows certain structures that behave as a single object. As a response to the applied ablation, these structures are moving together, thus revealing their connection. Resulting moving part comprises sister kinetochores, an intact sister k-fiber, a bundle of microtubules located between sister kinetochores and finally, the remaining stub as a leftover part of the cut sister k-fiber. According to text books, there is no direct interaction between sister k-fibers. A recent study revealed microtubule bundle between sister kinetochores as a structural component in the spindle which was named bridging microtubules [50; 69], (Figure 12). My interest is to understand this bundle, and with the mentioned observation following conclusion has been made: bridging microtubule bundle is connected to sister k-fibers via certain interactions that are still preserved after applied laser ablation. Main hypothesis is that it laterally connects sister k-fibers and contributes to distribution of forces in the spindle.

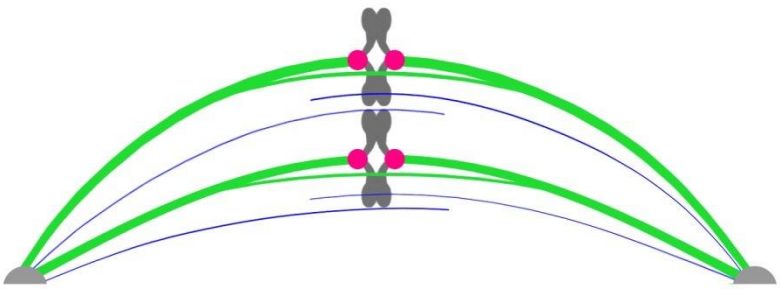


Fig 12. New model of the spindle with bridging microtubule bundle laterally connecting sister k-fibers. Note that the antiparallel composition of bridging bundle is not pointed out in this scheme.

It has already been shown recently that bridging microtubule bundle is composed of antiparallel microtubules. Since it has been proven that cross-linking protein PRC1 is located in the antiparallel region of the bridging microtubule bundle [50], I wished to affect its thickness by reducing the amount of PRC1. With this approach I would expect the force balance to be perturbed. Following analyses were conducted in treated cells: primary response to the cut, bridging microtubule bundle thickness and shape of the spindle. From measurements of the mentioned primary response, force balance in the spindle element was analyzed which was put in correlation with the bridging microtubule thickness. Shape was analyzed in order to extract the amount of forces acting at certain parts of the spindle.

Other approach was to observe microtubule dynamics in the cut part of the spindle. For this reason, HeLa cell line stably expressing EB3 fused to GFP was used. Within chosen time, with clear events occurring in the region between sister kinetochores, it would be possible to track individual growing microtubules. My hypothesis here is that it should be possible to observe comets passing between sister kinetochores, thus revealing the individual microtubules that grow in the bridging microtubule bundle. Since bridging bundle is composed of antiparallel microtubules, I additionally expect to see comets passing in opposite directions.

2. Materials and methods

2.1. Cell culture

HeLa-TDS cells were permanently transfected and stabilized using pEGFP-a-tubulin plasmid (courtesy of Mariola Chacon), which was acquired from Frank Bradke (Max Planck Institute of Neurobiology, Martinsried). Cells were grown in Dulbecco's Modified Eagle Medium (DMEM) (1 g/l D-glucose, L-glutamine, pyruvate) with 50 µg/ml geneticin (Life Technologies, Waltham, MA, USA), 10% fetal bovine serum (FBS, Gibco, Life Technologies) and 1% penicillin and streptomycin. The cells were kept in a Heracell humidified incubator (Thermo Fisher Scientific, Walthman, MA, USA) at 37°C and 5% CO_2. Cells were split and reseeded every 48-60 hours. Described cell maintenance was applied to all cell lines used in this study.
HeLa cells stably expressing 2xGFP-EB3 and CENPA fused to mCherry were permanently transfected with retroviral plasmid (courtesy of Julie Welburn). Cells have been checked for mycoplasma by Lonza luminometar and PCR and were myco negative.

2.2. Imaging and laser microsurgery

Prior to live cell imaging, medium was replaced with Leibovitz L-15 CO_2 independent medium (Gibco, Life Technologies) containing 10% FBS and 1% antibiotic mixture of penicillin and streptomycin. Imaging was performed with a Zeiss LSM 710 NLO inverted laser scanning microscope with a Zeiss PlanApo 63x/1.4 oil immersion objective (Zeiss, Jena, Germany) heated with an objective heater system (Bioptechs, Butler, PA, USA). Cells were maintained at 37°C in Tempcontrol 37-2 digital Bachhoffer chamber (Zeiss). For excitation, a 488 nm line of a multi-line Argon laser (0.45 mW, LASOS) and a helium-neon (HeNe) 594 nm laser (0.11 mW) were used for GFP and RFP respectively. The laser power used for excitation was in range 8-15% with a pinhole size 0.7 µm. The microscope was equipped with a QUASAR detector with 32 channels (Zeiss, Germany), which made it possible to image two emission bands in parallel: 490-561 nm for GFP and 588-694 nm for RFP fluorescence. Laser microsurgery was performed on the outmost k-fiber in a user defined region of interest (ROI) by means of a single Ti:Sa femtosecond pulsed laser (Chameleon Vision 2, Coherent), set to 800 nm wavelength. During laser ablation, no images were acquired. For RNA interference

experiment, time lapse Z-stacks of 6 optical planes with a 500 nm step were taken at 2.5-5 second interval with averaging of four scans. For EB3 experiment, time laps Z-stacks of 2 optical planes were taken at 0.6-1 second interval with averaging of either 1 or 2 scans. The system was controlled by ZEN 2011 software (ZEISS, Germany).

2.3. RNA interference

2.3.1. Transfection and sample preparation

Cells were transfected by electroporation using Nucleofector Kit R with the Nucleofector 2b Device, using the high-viability O-005 program (Lonza, Basel, Switzerland). The following protocol was used: cells at approximately 60% con-fluency were trypsinized for 5 minutes. Counting of cells was performed in Neubauer improved chamber and 1 million cells were collected and centrifuged for 5 minutes at 1000 rpm at room temperature. Medium was removed and cells were resuspended in nucleofector solution containing 200 nM siRNA constructs (targeting, SiGENOME smart pool, Human PRC1 or nontargeting, SiGENOME control pool, nontargeting #1, Dharmacon) together with 2 μg of mRFP-CENP-B (kinetochore protein) plasmid (pMX234) provided by Linda Wordeman (University of Washington School of Medicine). Cells in nucleofector solution were collected and placed in a plastic cuvette that was inserted in the nucleofector machine and the appropriate program was applied. Transfected cells were seeded in 35 mm poly-d-lysine coated glass coverslip dishes (MatTek Corporation, Ashland, MA, USA) in different concentrations (high, medium, low). Prior to imaging cells were synchronized in the same dishes. Cells were incubated in thymidine (Sigma-Aldrich, St. Louis, MO, USA) at final concentration 2 mM for 17 hours. Cells were then washed 3 times with warm phosphate buffered saline (PBS) and left in DMEM medium with supplements for ~3 hours. After incubation, Cdk1 inhibitor RO-3306 (Calbiochem, Merck Millipore, Billerica, MA, USA) was added at a final concentration of 9 μm and were incubated in RO-3306 for ~6 hours. After washing 3 times in warm PBS cells were left in the incubator with 2 ml DMEM medium to recover. Finnally, cells were arrested in metaphase by using proteasome inhibitor MG-132 (Sigma-Aldrich, St. Louis, MO, USA) at 20 μm concentration. The imaging was performed in L-15 medium and MG-132 ~20 minutes after adding MG-132 as described, 72 hours after transfection.

2.3.2. Image analysis

All image precessing was performed in ImageJ (National Institute of Health, Bethesda, MD, USA) and MatLab (MathWorks, Natick, USA). Successfulness of applied ablation was determined by at least one of the following characteristics: outward movement was clear enough; interkinetochore distance changed obviously after performed microsurgery; the gap that is formed on the cut k-fiber was getting spread towards the spindle pole it originates from.

2.3.2.1. Velocity of outward movement

Cut spindle element moves outward with certain velocity. Kinetochores were tracked using Low Light Tracking Tool, an ImageJ plugin [70]. The kinetochores were tracked in xy-plane within individual imaging planes. The start and end times of the outward movement were manually selected. Initial position and maximum displacement were observed as a change in movement during certain time. This data was used for calculating mean velocity of outward movement. Velocity of the outward movement was measured in siRNA treated cells as well as in nontargeting control cells.
Percentage of change in interkinetochore distance was extracted from the tracking data performed with the Low Light Tracking Tool.

2.3.2.2. Bridging fiber thickness

Intensity of the signal between kinetochores was measured with a 3-pixel thick line tool between outermost sister kinetochores in the cut spindle element that was perpendicular to the line joining the two sister kinetochores. Intensity profile was taken along this line and the mean value of the background cytoplasm signal was subtracted from it. The signal intensity of the bridging fiber was calculated as the area under the peak closest to the kinetochores. The intensity of the k-fiber signal was measured 1 μm away from one of the sister kinetochores.

2.3.2.3. Spindle shape

Using multipoint tool, the shape of an ablated spindle element was tracked before and after microsurgery. At time point before ablation, tracked line was extending from one spindle pole along intact k-fiber until first sister kinetochore. The gap between sister kinetochores was not tracked in order to know their position. After the gap, tracking was continued along following sister k-fiber (to be cut) to finally meet other spindle pole. This measurement gives us the contour of a spindle element which makes it possible to extract robust parameters like spindle length (distance between two spindle poles) and width (distance between sister kinetochore pair in the spindle element and the axis connecting two spindle poles), angle on the centrosome and angle at kinetochores. The two angles were calculated by fitting a line through 3 points on the measured contour of the spindle element. The angle of tracked k-fiber in the vicinity of the centrosome and the angle of the k-fiber in the vicinity of the kinetochore enable us to determine and calculate the amount of force acting on centrosome and the amount of force acting on kinetochore. After ablation, continuous change in the contour was measured during 3 time frames after it was applied in order to extract the straightening of the cut spindle element.

2.3.3. Polyacrylamide gel electrophoresis and Western blot

Transfected cells at 80% confluency were lysed in RIPA (radioimmunoprecipitation assay buffer, ENZO life science, Germany) lysis and extraction buffer with protease inhibitors (complete protease inhibitor cocktail tablets, Roche, Germany) as recommended by the manufacturer. Concentration of isolated proteins was measured using BCA (bicinchoninic acid assay) protein assay kit (Pierce Biotechnology, USA). Proteins were denatured by the combination of SDS (sodium dodecyl sulfate) and beta-mercaptoethanol in the loading buffer. Lysates were cooked for 10 minutes at 95°C and separated by SDS-PAGE (sodium dodecyl sulfate polyacrylamide gel electrophoresis, NuPAGE 10-well 4-12% Bis-Tris gels, Invitrogen, USA; 120 V, 2hrs). Separated proteins were transferred to nitrocellulose membrane (15 V, o/n) and analyzed by western blot with primary monoclonal anti-PRC1 (1:1000 in 5% milk) and anti-GAPDH antibodies (1:500 in 5% milk). Rabbit polyclonal anti-PRC1 (protein

regulator of cytokinesis 1) antibody (H-70) (Santa Cruz Biotechnology, USA) was used for PRC1 detection and a Mouse monoclonal anti-GAPDH (glyceraldehyde 3-phosphate dehydrogenase) antibody (0411) (Santa Cruz Biotechnology, USA) was used for detection of GAPDH. Membrane was then incubated in secondary polyclonal anti-mouse and anti-rabbit antibodies (1:5000 in 5% milk) for 2 hours. Proteins were visualized by chemiluminescence, with ECL (enhanced chemilumescence, GE Healthcare, USA) and SuperSignal West Dura (Thermo Scientific, USA) used as chemiluminescence substrates for detection of HRP (horseradish peroxidase) conjugated antibodies. Detection was conducted on Amersham Hyperfilm ECL films (GE Healthcare, USA), which were then scanned.

2.3.4. Immunocytochemistry

Immediately after imaging, cells were fixed in ice-cold methanol (100%) for 3 minutes and washed. In order to permeabilize cells membranes, cells were incubated in triton (0.5% in phosphate buffer saline (PBS)) for 25 minutes at room temperature softly shaken. Unspecific binding of antibodies was blocked in blocking solution (1% normal goat serum in PBS) for 1 hour on 10°C softly shaken. Cells were incubated in 250 µl of primary antibody solution (1:50 in 1% normal goat serum (NGS) in PBS) for 48 hours at 10°C. Rabbit polyclonal anti-PRC1 antibody (H-70) (Santa Cruz Biotechnology, USA) was used. After washing of primary antibody solution, cells were incubated in 250 µl of secondary antibody solution (1:500 in 2% NGS in PBS; A21430, Alexa fluor 555 F (ab') 2 fragment of goat anti-rabbit IgG (H+L), molecular probes, USA) for 1 hour at room temperature softly shaken and washed. After washing of the secondary antibodies, cells were incubated in a DAPI solution (1:1000 in PBS) for 5 minutes at room temperature and washed. After each incubation step, washing was performed three times for 5 minutes in PBS softly shaken at room temperature. Successfulness of performed protocol was eventually analyzed under the microscope Zeiss LSM 710 NLO inverted laser scanning microscope (Zeiss, Jena, Germany).

2.4. Image analysis in EB3 experiment

Video material of cells with applied microsurgery was chosen for analysis of the growing microtubules in the bridging microtubule bundle depending on the following criteria: outward movement of the cut spindle element should preferably be strong enough so as to distinguish EB3 comets growing in the k-fiber and continuing along the region between sister kinetochores; certain spindles with less pronounced response to the cut were not rejected if it was possible to clearly describe the events occurring in the spindle element. Further on, in video material of cells that met the chosen criteria, certain time with clear events in the cut spindle element was selected. Videos were analyzed in ImageJ either by eye, making montage of the selected time or finally by visualizing microtubule dynamics during selected time by using kymographs. Velocity of the growing microtubules was measured by using the line tool extending from initial comet position until the point where it is still visible/distinguishable. Comets used for measuring velocity were tracked for at least 4 time frames (~2.8-3 seconds).

3. RESULTS

3.1. Set up for microscopy and interpretation of laser microsurgery

HeLa cell lines used in this research express different proteins of interest fused with fluorescent markers (e.g. green fluorescent protein (GFP), mCherry, red fluorescent protein (RFP)). I was interested in the mitotic spindle and the localization of different proteins in that machinery helps us understand its structure and composition. Since we visualize proteins with different localization and behavior, properly assembled and unperturbed spindles, when mutually compared, may appear morphologically different, but the spindle is convex with length defined as the axis connecting two spindle poles, whilst the axis connecting two opposite outermost sister kinetochore pair determines the spindle width.

Microscopy, as a method that enables us to study living cells, combined with different types of experiments conducted in cell lines with fluorescently labeled proteins, teaches us about their role in spindle architecture and performance. For live cell imaging I used laser scanning microscope equipped with Ti:Sa (Titanium:Sapphire) femtosecond pulsed laser (Chameleon Vision 2, Coherent) that was used for performing laser microsurgery (further also referred to as “cut” or “(laser) ablation”) on the outermost k-fiber, i.e. on one of the sister k-fibers bound to sister kinetochore pair which is the furthest from the axis connecting two spindle poles. This structural component was named the spindle element and it consists of sister kinetochore pair and all its bound microtubules (Figure 13).

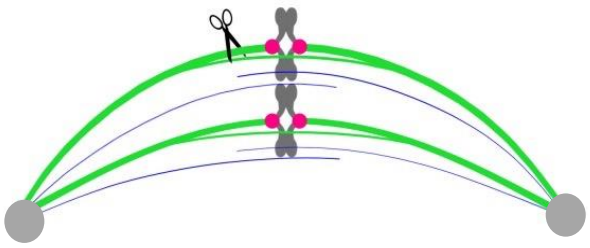


Figure 13. Scheme of the spindle element with scissors indicating the position of the laser microsurgery. Chromosomes and spindle poles are depicted in gray color, kinetochores are shown in magenta, k-fibers in green and antiparallel microtubules in blue color. One spindle element extends from one spindle pole to the opposite one, and it comprises two sister kinetochores and all coupled microtubules (e.g. two sister k-fibers).

I was particularly interested in proteins tubulin, PRC1 and EB3, which have distinct roles in the spindle. In addition to selected, labeled protein of interest (tubulin and EB3), all HeLa cell lines used in this study, were transfected with a sequence coding for fluorescently labeled kinetochore protein. HeLa cell line stably expressing tubulin-GFP was transfected with mRFP-CENP-B plasmid, and was used to study force distribution in the mitotic spindle, whilst HeLa cell line stably expressing 2xGFP-EB3 and the kinetochore protein CENP-A fused with mCherry was used to study microtubule dynamics. By visualizing kinetochores it was possible to set the position of the cut and to observe their behavior as a response to the applied ablation. For conducting the laser microsurgery experiment, cells were chosen depending on the signal intensity of the fluorescently labeled proteins of interest. In particular, only cells that were expressing labeled kinetochore protein and labeled protein of interest (tubulin or EB3) were selected for imaging. The signal intensity in chosen spindles was preferably in the range from medium to strong. Additionally, the phase of mitosis for performing laser microsurgery was chosen depending on the alignment of kinetochores in the metaphase plate. If chosen criteria have been met, laser microsurgery was performed on the outermost k-fiber. In my experiments, all cells with multipolar spindles, as well as ones in which the spindle was tilted in the z-direction, were discarded for acquiring video material.

Now let's describe the possibilities, which are given to us through laser ablation. The laser ablation performed in the selected spindle element reveals its mechanical properties. The position of the cut was in my experiment set in vicinity of one of the sister kinetochores rather than in the proximity of the spindle pole. The response to applied ablation enlightened my understanding on forces acting in the spindle. With this approach, the system was perturbed in a way that these forces became released and this event opened possibilities for describing spindle mechanics. Performed laser ablation mostly resulted in movement of the cut spindle element which is in correlation with the force present within. In addition to this basic response, mentioned movement clears up the composition of the cut part of the spindle, thus exposing the structural components present within. Since the spindle is structurally complex, ablation turned out to be an important approach in analyzing single spindle element resolved from the neighboring ones. In both cell lines, the outermost k-fiber in z-position was selected for ablation because the spindle element thus predominantly moved in the x,y-plane. To consolidate, the response to laser ablation revealed structural components of the cut part of the spindle, and by analyzing the response it was possible to describe the force distribution in the spindle.

When it comes to forces, laser microsurgery results in two distinct responses which occur within seconds after it was performed. One is the outward movement (movement away from the center of mass of the spindle) of intact part of the cut spindle element — two sister kinetochores move together with the k-fiber that is still connected to one spindle pole and with the microtubule bundle located between two kinetochores. When thoroughly analyzed, this response can reveal a lot about force that acts in the spindle element. The outward movement suggests presence of compressive force acting at certain part of the spindle element and release of this force after microsurgery. This observation was expected since the bent shape of the spindle element suggests that it is compressed. By measuring the velocity of sister kinetochore movement, it was possible to determine the amount of compressive force, or at least to determine the difference between differently perturbed spindles. The other response is a decrease in distance between two sister kinetochores that lost the connection to one pole. This response mostly started occurring immediately after successful cut or simultaneously with the outward movement and it suggests presence of a tensile force acting on sister kinetochores and its release after microsurgery [72; 73]. Once the connection to one pole is lost, centromeric region is no longer stretched. Thus the decreased distance between sister kinetochores indicates establishment of the relaxed state. Described, concurrent events are defined as the primary response that is the result of forces being released after successful laser microsurgery (Figure 14). In HeLa cell line expressing tubulin-GFP and mRFP-CENP-B, resulting moving spindle element comprised sister kinetochores, an intact sister k-fiber, a bundle of microtubules located between sister kinetochores and a stub as a leftover part of the cut k-fiber (Figure 15). On the other hand, in HeLa cell line expressing 2xGFP-EB3 and mCherry-CENP-A, the cut spindle element was observed as movement of the sister kinetochores, whilst the comets of green signal that correspond to growing microtubule plus-ends were observed throughout the spindle (element) in astral, antiparallel and kinetochore microtubules (Figure 16). These two primary responses teach us about the counterintuitive force map in the spindle element, which we believe is distributed in a similar manner throughout all spindle elements.

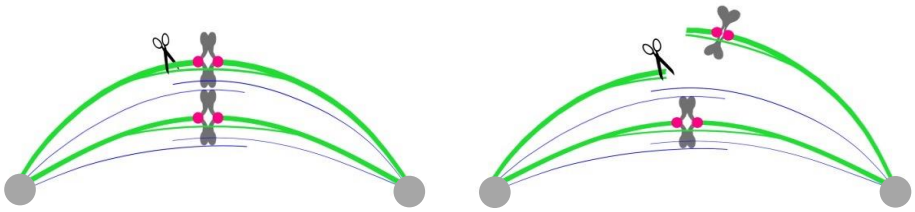


Figure 14. Scheme of the position of the laser ablation in the spindle element and the primary response. Severing of the outermost k-fiber results in release of compressive force in the spindle element (outward movement) as well as release of tensile force acting on sister kinetochores in the cut spindle element (decreased interkinetochore distance). The primary response depicted in the scheme as seen in HeLa cell expressing tubulin-GFP (green) and mRFP-CENP-B (magenta).

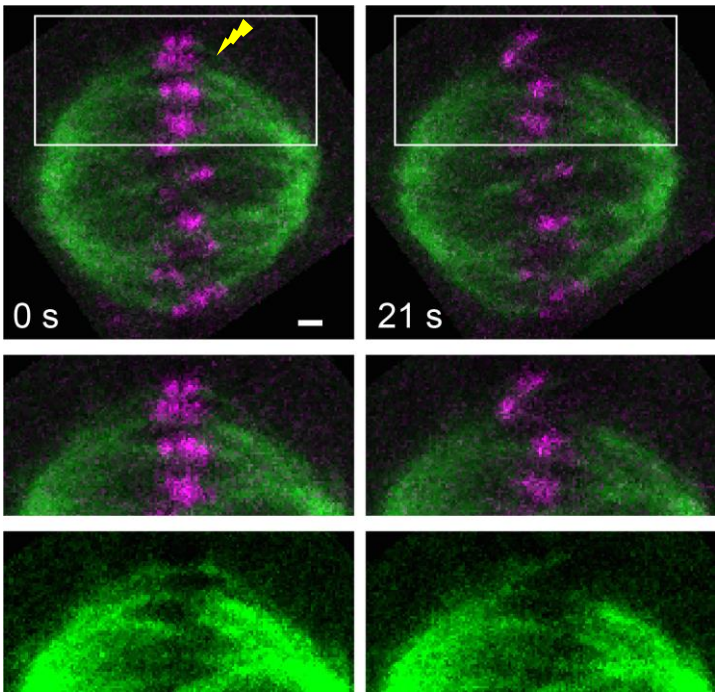


Figure 15. Image of mitotic spindle in HeLa cell expressing tubulin-GFP (green) and mRFP-CENP-B (magenta) acquired with laser scanning microscope. Laser ablation reveals structural components in the spindle element: intact k-fiber, sister kinetochores, bundle between sister kinetochores and a stub as a leftover part of the cut k-fiber that is still connected to the sister kinetochore that was closer to the ablation point. White bar represents 1 μm scale.

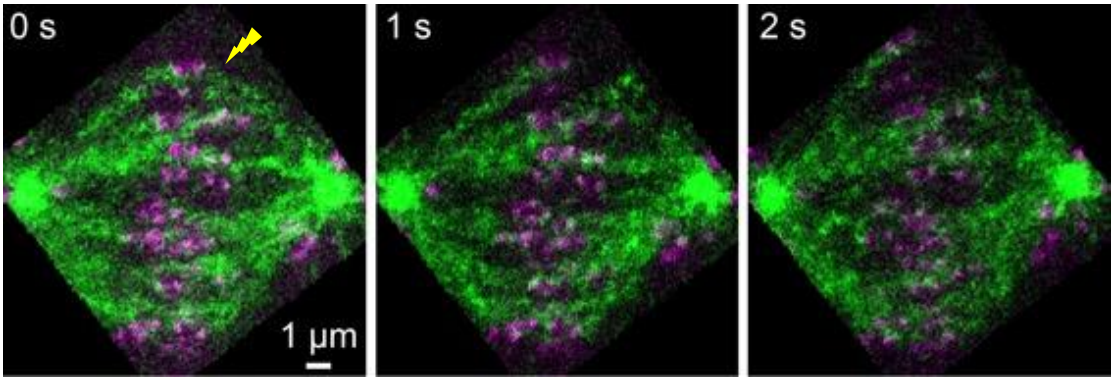


Figure 16. Laser ablation outcome as observed in HeLa cell line stably expressing 2xGFP-EB3 (green) and mCherry-CENP-A (magenta). The comets of green signal make the contour of the spindle. With applied ablation it was possible to analyze the microtubule dynamics in the region between sister kinetochores. As seen in pictures, majority of comets are observed in k-fibers and antiparallel microtubules. However, when analyzing a small region between sister kinetochores, many astral microtubules were observed passing in their close vicinity. For this reason, only time frames with clear region around sister kinetochores were selected for analysis. White bar represents 1 µm scale.

Successfulness of applied ablation was in my experiments determined by at least one of the following characteristics: outward movement was clear enough; interkinetochore distance changed obviously after performed microsurgery. In addition to these criteria set both in EB3 and RNAi experiment, an additional criterion was set in RNAi experiment: the gap that is formed on the cut k-fiber was getting spread towards the spindle pole it originates from. This additional criterion hasn't been set in EB3 experiment since my primary intension wasn't to visualize fluorescently labeled microtubules nor to analyze the mechanics of the primary response in this experiment, but rather to observe clear events in the region of interest.

3.2. Self-repair mechanism

To fortify, cut spindle element consists of the intact k-fiber, sister kinetochore pair, the bridging bundle and a remaining stub as a part of the cut k-fiber that is still bound to sister kinetochore which was closer to the ablation point. After the primary response, secondary response takes place. Recent study described a self-repair mechanism of the spindle that takes place soon after the outward movement reaches its amplitude [47]. It was usually observed as movement of the cut spindle element in reverse direction of the direction of the outward movement. In one scenario this movement towards spindle's center of mass resulted in reconnection and reintegration of the cut spindle element to the spindle. If it occurs in opposite direction of the outward movement, the reconnection results in reestablishment of forces that were present in the spindle element before the ablation was applied, and it was observed as restoration of a tensile force on sister kinetochores. If one would look at the reintegrated spindle element that was reconnected in this way, it would be impossible for observer to determine position of the cut and to perceive that it was recently performed (Figure 17). In other scenario, the spindle element was reconnected in a way that the stub got pulled to a totally different position with respect to the position of the spindle element before the cut. In certain cases observed in this study, the sister kinetochore pair sometimes twisted either inwards (Figure 18) or backwards (Figure 19) and got pulled towards the spindle pole it is still connected to. Secondary response occurred in all cell lines used in this study and it was observed in ~82 % (63 cells) of analyzed cells (in RNAi and EB3 experiment). In analyzed cells were it was not observed, an acquired video material was too short and the secondary response has not begun during the acquired time frames.

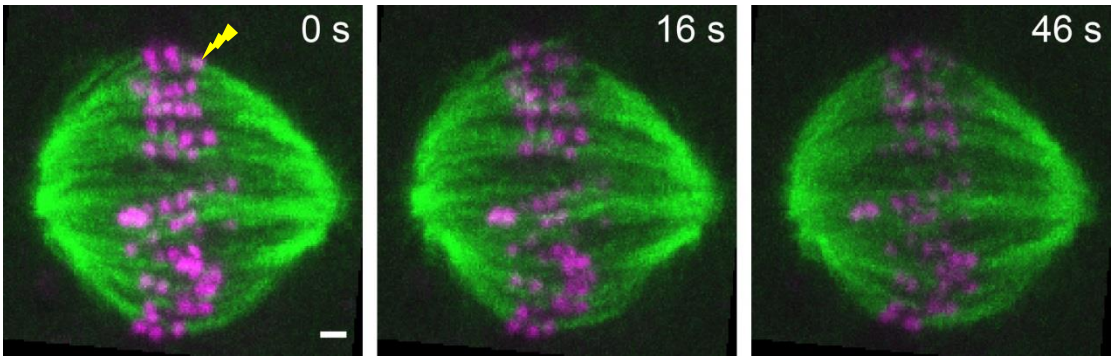


Figure 17. Secondary response with "healthy" reconnection as seen in HeLa cell line expressing tubulin-GFP (green) and mRFP-CENP-B (magenta). ~45 seconds after applied ablation, the cut spindle element, as seen in the third image, is fully integrated in the spindle with restored tensile force at kinetochores. White bar represents 1 μm scale.

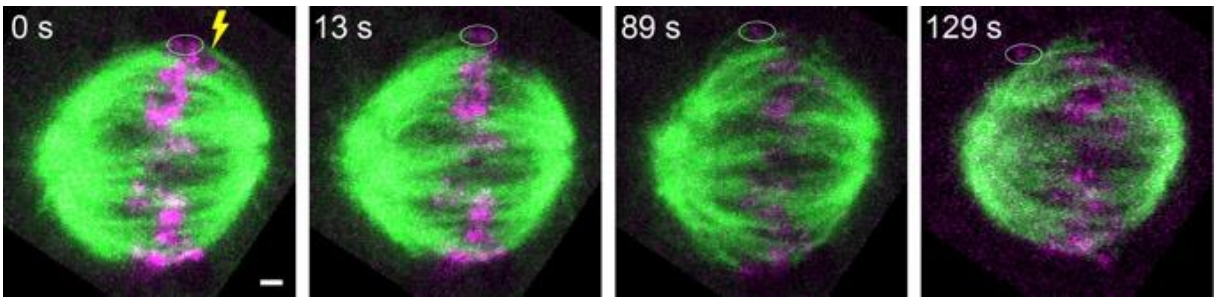


Figure 18. Secondary response in HeLa cell line expressing tubulin-GFP (green) and mRFP-CENP-B (magenta). At 13 seconds (s) time point the outward movement takes place, and at 89 seconds (s) time point the mechanism of secondary response is pulling the cut spindle element towards the pole it is still connected to. In this image sister kinetochores twisted inwards and were transported to the spindle pole. Sister kinetochore with bound stub twists in the direction towards spindle's center of mass. White bar, 1 μm.

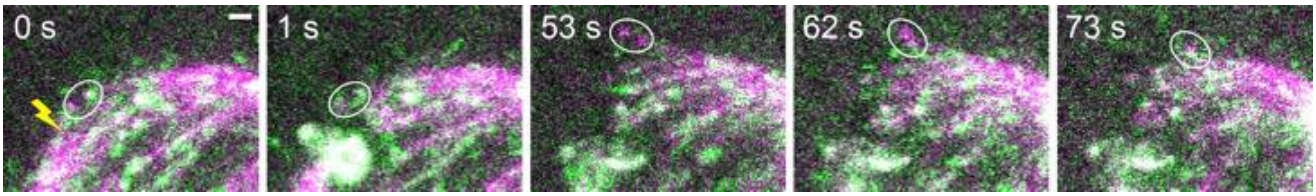


Figure 19. Secondary response in HeLa cell line stably expressing 2xGFP-EB3 (green) and mCherry-CENP-A (magenta). Sister kinetochore with bound stub twisted outwards (in the direction away of the spindle's center of mass) and was pulled to the spindle pole. White bar, 1 μm.

3.3. Construction of a cell model for spindle analysis - PRC1

The greatest motivation for studying basic spindle architecture was the mostly consistent composition of the cut spindle element that was observed by Janko Kajtez and Anastasia Solomatina in group of Iva Tolić (Max Planck institute of molecular cell biology and genetics, Dresden). These observations and recently conducted experiments revealed the bundle between sister kinetochores as a novel structural component in the mitotic spindle. It is a bundle of antiparallel microtubules that laterally connects two sister k-fibers, and it was named the bridging microtubule bundle [50; 69]. This bundle is located in close vicinity of sister kinetochores (typically underneath kinetochores), and there is a strong evidence for its role in balancing forces in the mitotic spindle. Since described primary response teaches us about the two opposing forces that act simultaneously in a single spindle element, one cannot help but wonder how they are balanced. The bridging microtubule bundle, which came into focus as a mechanical link between sister k-fibers, indeed could participate in force distribution in the spindle. Even though the only reliable approach in understanding forces was to analyze the primary response in a single outermost spindle element, we believe that the bridging bundle is found in all spindle elements with consistent role. In addition to analysis of the primary response, I measured the thickness of the bridging bundle as described in chapter "Materials and methods".

Good approach in describing the hypothesized role of the bridging bundle in force balance was to affect its composition. Solomatina and Kajtez recently showed that they understood the system in a way that they could perturb it by changing the expression levels of chosen proteins [50; 69]. Since they hypothesized that the bridging bundle is composed in an antiparallel manner, they were interested in determining a cross-linking protein that is found in the bridging bundle. That protein turned out to be PRC1 (amongst others yet to be defined) and the laser microsurgery in their experiments resulted in the previously described primary response. In HeLa cell line stably expressing PRC1-GFP and transiently mRFP-CENP-B, we visualize the spindle midzone, which is in agreement with localization of the PRC1 protein. In the outermost spindle element, sister kinetochores are positioned in immediate proximity of the PRC1 signal and the laser ablation in their experiment revealed that the antiparallel bundle is moving together with sister kinetochores in the cut spindle element. This observation indicates that microtubules in the bridging bundle emanate from opposite poles and are mutually met in the equatorial region of the spindle where they form the antiparallel bridging

bundle. Their perturbation experiment was focused in increasing the thickness of antiparallel regions in the spindle. In HeLa cell line overexpressing PRC1 and tubulin, laser ablation was applied and analysis of outward movement and bridging bundle thickness was conducted. Their experiments motivated me to perturb the system in the opposite way by producing cells with decreased expression of PRC1 (decreased tehickness of the bridging bundle) and thus confirm that the bridging bundle balances forces in the mitotic spindle.

3.3.1. Analysis of laser ablation in PRC1-depleted cells

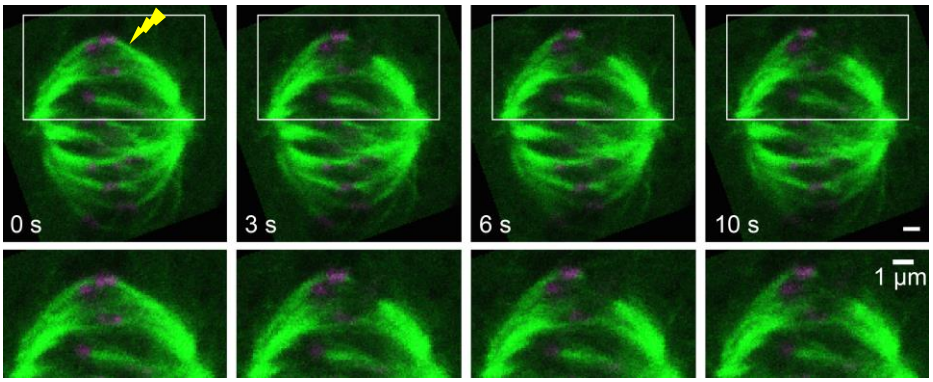
I hypothesized that by reducing the bridging bundle thickness, it would be possible to achieve less pronounced primary response. I used RNA interference to reduce the level of PRC1 protein which would result in decrease of the antiparallel regions (their thickness and/or length) in the spindle. I expected the knockdown to affect the bridging bundle thickness, and that the outward movement would be in correlation with the reduced thickness. This experiment was performed in HeLa cell line stably expressing tubulin-GFP, and was controlled by nontargeting siRNA. Nontargeting siRNA constructs are unmodified siRNA duplexes used as negative control. Cells treated with nontargeting control are used to reflect a baseline cellular response that can be compared to the cells that have been treated with target-specific siRNA. In treated cells I measured the bridging bundle thickness, velocity of the outward movement, change in interkinetochore distance and spindle shape. Since tubulin is a microtubule subunit, in this cell line microtubules are visualized as continuous green signal in kinetochore and antiparallel microtubules, whilst astrals are usually more or less apparent. Due to overlapping signals of k-fibers and antiparallel microtubules, laser ablation in this experiment also clears up components in the cut spindle element, as recently described. Analyses conducted in my RNAi experiment were led by the same idea that motivated Kajtez and Solomatina. For this reason, chosen results will be presented side by side in same graphs and thus directly compared.

In RNAi treated cells, laser ablation was performed as described in section 2.2. “Imaging and laser microsurgery” of “Materials and methods” and 3.1. “Proteins of interest, microscopy and laser microsurgery” of this chapter. The outermost spindle element was selected in the imaging z-plane and the laser ablation was performed on one of two sister k-fibers. Applied

severing of the k-fiber would result in perturbation that would teach me about the mechanical properties of the cut part of the spindle. Compared to my control cells and recently conducted experiments by Solomatina and Kajtez, the results revealed whether the spindle mechanics has been perturbed in my experiment.

Once performed, successful laser ablation results in release of compressive force in the spindle element and in a release of tensile force acting on sister kinetochores (Figure 20 a)). Release of tension is observed as decreased interkinetochore distance and it was one of the criteria that determined the successfulness of performed ablation. The amount of tensile force wasn't quantified in my analysis, but was rather used to show that it was in average released after performing laser microsurgery. For analysis I chose 48 spindles with at least one of the criteria for successful ablation satisfied. Percentage of change in interkinetochore distance was extracted from the tracking data performed with the low light tracking tool (Figure 20 b)). Analysis of the release of tensile force revealed that interkinetochore distance decreased in ~85% (41 cells) of analyzed cells. In ~6% (2 cells) it was impossible to perceive the change in interkinetochore distance due to overlapping signal with neighbouring kinetochores in time frames before ablation. In ~10% of cases (5 cells) the distance between kinetochores didn't decrease, and the successful cut was determined by at least one of the remaining criteria.

a)



b)

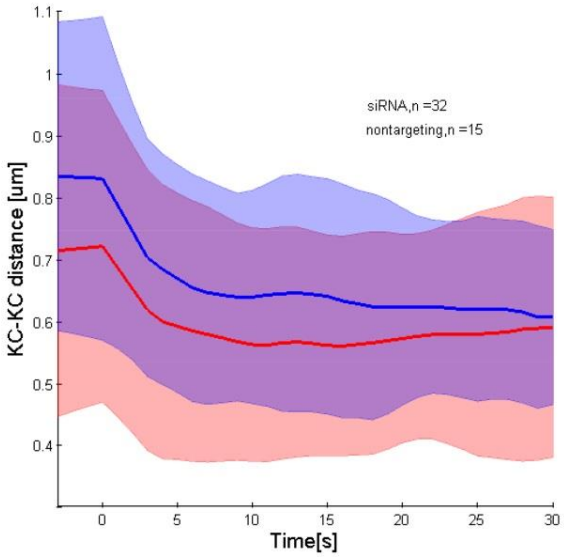


Figure 20. a) Primary response in HeLa cell line expressing tubulin-GFP (green) and mRFP-CENP-B (magenta). White bar represents 1 µm scale. b) Interkinetochore distance (KC-KC distance) in the cut spindle element was measured in time frame before the ablation (value "0" on x-axis) and was tracked continuously during the following time frames, for each spindle with met criteria of successful cut. Red (PRC1 siRNA) and blue (nontargeting control) lines are given as mean values of continuous change in interkinetochore distance with corresponding light red and light blue area marking standard deviation.

Cut spindle element moves outwards with certain velocity which is in strong correlation with the amount of compressive force acting in the spindle element. Kinetochores were tracked during 3 time frames after ablation (~9 sec.) using Low Light Tracking Tool. I observed the outward movement (more or less pronounced) in ~83% (40 cell) of all analyzed cells. In 12% (6 cells) of cases I observed no outward movement, and in 6% (3 cells) of cases the sister kinetochores moved inwards (towards the spindle's center of mass). The velocity of their (outward) movement was measured in PRC1 siRNA treated cells, as well as in nontargeting control cells (Figure 21). I expected for the data measured in nontargeting control cells and PRC1 siRNA to be mutually significantly different. In particular, the velocity of outward movement should have been lower in our PRC1 siRNA treated cells when compared to nontargeting control cells. Regardless of predicted outcome, the velocity of outward movement in PRC1 siRNA treated cells is only slightly lower in comparison to control cells. I assume that the chemicals used in my synchronization protocol affected the response to ablation.

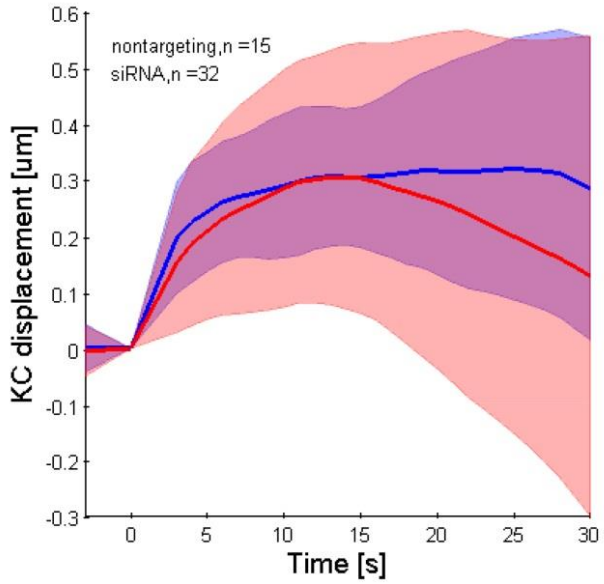


Figure 21. Average outward movement (KC displacement) as measured in siRNA treated cells (thin red line) and nontargeting control cells (thin blue line). We were interested in first response that occurs within seconds after performing laser ablation (x axis). On y axis is the displacement of sister kinetochore that was closer to the ablation and its movement was tracked as displacement in y axis, which describes movement of sister kinetochore away from spindle's center of mass. Light red area (PRC1 siRNA) and light blue area (nontargeting) are represented as standard deviation.

Cells used in RNAi experiment were synchronized prior to imaging. The synchronization protocol was successful in a way that spindles appeared healthy and weren't tilted in the z-direction. However, drugs used to arrest cells in metaphase are in certain ways affecting mitotic spindles. It would be more preferable not to use them in order to reduce the treatment of cells. I observed several merotelic attachments of kinetochores in synchronized cells, which affected the outward movement velocity as well as the possibility for the outward movement to reach its amplitude that would usually depend on the amount of compressive force in the spindle element. Merotelic orientation is an error that occurs in connection of sister kinetochores. In this case one kinetochore in sister kinetochore pair is attached to microtubules emanating from opposite poles of the spindle. The comparison of primary response between my control cells and tubulin-GFP cell line will be pointed out in this section where my synchronized cells will be plotted on the same graph with the results of Kajtez and Solomatina measured in control cells (HeLa cell line expressing tubulin-GFP and mRFP-CENP-B). My nontargeting control cells and PRC1 siRNA treated cells had similar outward movement in comparison to HeLa cell line stably expressing tubulin-GFP that was used as a control in Kajtez and Solomatina experiment (Figure 22).

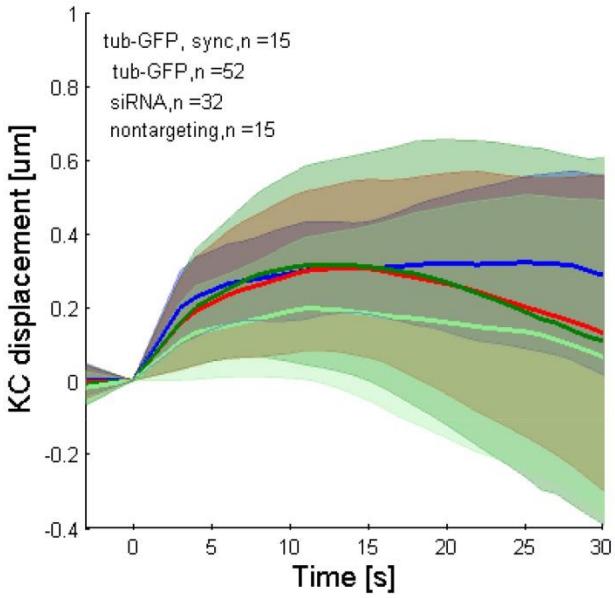


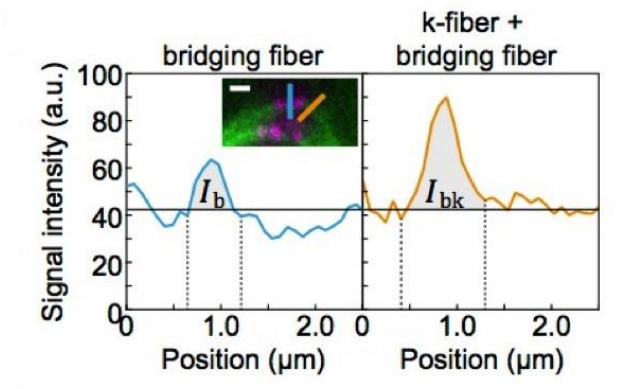
Figure 22. Kinetochore displacement in PRC1 siRNA treated cells (thin red line), nontargeting treated cells (thin blue line), unsynchronized tubulin-GFP control cells (thin green line, [62]) and in synchronized tubulin-GFP cells (thin light green line) by Kajtez and Solomatina, [50; 69]. Light areas with coupled colors of the thin lines are given as standard deviation.

3.3.2. Analysis of bridging bundle thickness

In order to determine the correlation between bridging bundle composition and outward movement, I measured thickness of the bridging bundle. Measured intensity of the signal between kinetochores was interpreted as bridging microtubule thickness. Amongst 48 analyzed cells, both PRC1 siRNA and nontargeting, the bridging bundle was observed by eye in ~64% (31 cells) of cut spindle elements. In ~25% of spindle elements (12 cells) bridging bundle hasn't been observed by eye, and in ~8% of cases (4 cells) it was impossible to distinguish the cut spindle element from the neighboring ones. To estimate the ratio between bridging microtubule bundle and k-fiber, the signal intensity of k-fiber was also measured. This measurement was done in proximity of one of the sister kinetochores, on the side facing the spindle pole (Figure 23. a)). Measured thickness ratio bMT/k-fiber is 20±14 % for nontargeting (15 cells) and 14±14 % for PRC1 RNAi (26 cells). From this measurement it was estimated that bridging bundle contains 25% of microtubules in the k-fiber in nontargeting control cells, and 16% in cells with reduced levels of PRC1. When put in correlation with previously measured data of k-fiber thickness obtained with electron micrographs (17±2 microtubules in k-fiber [74]), my data indicates that there are 3±1 microtubules contained within thinner bridge. In addition to difference in the primary response, the measured ratio between k-fiber and bridging bundle thickness was bigger in nontargeting control cells used in my experiments, than in control cells used in Kajtez and Solomatina experiment. MG132 (carbobenzoxy-Leu-Leu-leucinal) is a potent protease inhibitor (one of the chemicals used in our synchronization protocol) that was used to arrest cells in metaphase so as to achieve the same phase of mitosis in cells chosen for further experiments. It is possible that once the metaphase is prolonged more microtubules grow in the k-fiber thus making the measured ratio between k-fiber and bridging bundle bigger. Since the measured ratio revealed such unintentional perturbation, it was expected for the outward movement to depend on these conditions and it indicated that compression was affected and that it modulates the outward movement.

Even though measured difference isn't pronounced, thickness data can be put in correlation with the outward movement (Figure 23. b)). T-test (performed in MatLab) of comparison between PRC1 siRNA and nontargeting treated cells revealed the p-value: p=0,186 which indicates that the difference isn't significant. When compared to tubulin-GFP cells line, calculated p-value of the t-test is p=2,641 * 10^(-12) for PRC1 siRNA, and for nontargeting control cells is p=2,829 * 10^(-7), thus not revealing significant difference.

a)



b)

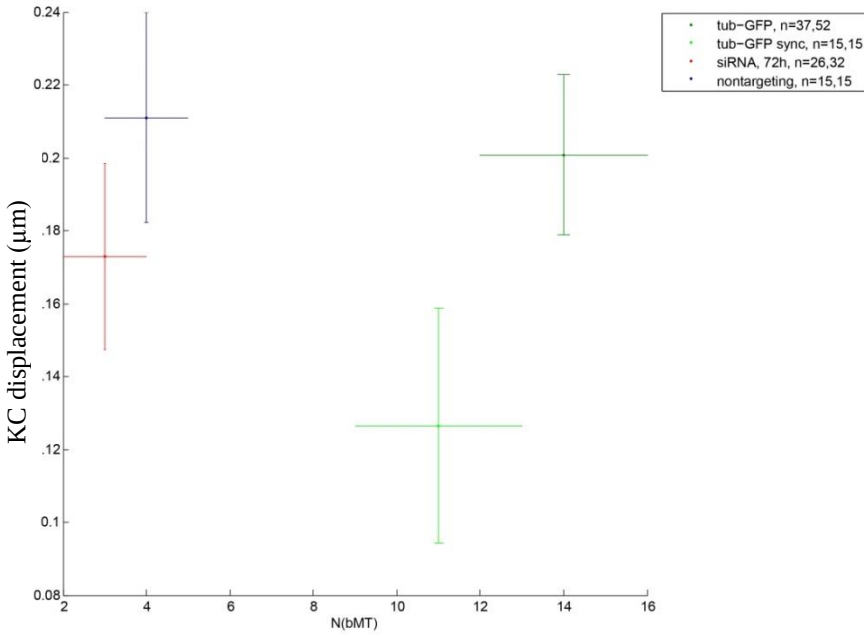


Figure 23. a) Scheme of measurements of thickness ratio bMT/k-fiber as performed in PRC1 siRNA and nontargeting treated cells. Blue line represents measurement and plot (blue) of signal intensity of the bridging bundle, whilst the yellow line and plot represent measurement of signal intensity of k-fiber and bridging bundle ("a.u." stands for arbitrary units). Measurements are performed as described in section "Materials and methods". White bar represents 1 μm scale bar. b) Plot of measured data of outward movement and thickness of the bridging bundle. "N(bMT)" corresponds to the number of microtubules in the bridging bundle and "KC displacement" corresponds to the change in the position of kinetochore that was closer to the ablation site in y axis and it was measured in first time frame after ablation. For number of cells, first set of values in the legend ("tub-GFP", N=37 for tubulin-GFP cell line, "tub-GFP sync", N=15 for synchronized tubulin-GFP cell line, "siRNA, 72h", N=26 for PRC1 siRNA treated cells, "nontargeting", N=15 for nontargeting control cells) corresponds to x-axis, whilst second set of values corresponds to y-axis. Since thickness could not be measured in all cells due to the overlapping of signal in the bridging bundle with the signal of neighboring microtubules, some cells had to be eliminated from thickness measurement.

3.3.3. Analysis of the spindle shape

Spindle element, in which the ablation was performed, was tracked with multipoint tool in ImageJ (National Institute of Health, Bethesda, MD, USA). This measurement was conducted in a time frame before ablation and in three time frames after the k-fiber has been severed. Points set along the outermost sister k-fibers give us the contour of a chosen spindle element. In intact spindle element (time frame before the applied ablation) these measurements can be analyzed in a way that it is possible to extract the values of spindle length (distance between first and last point in the analyzed contour, i.e. distance between spindle poles) and half-width (distance between the axis connecting first and last point in the analyzed contour and the axis connecting first and last point in the gap between sister kinetochores), (Figure 24). Measured average value of spindle length is 11.6±1.3 μm in PRC1 siRNA treated cells (32 cells), and the average spindle length in nontargeting treated cells 12.2±1.7 μm (15 cells). In same cells measured average value of the spindle half-width is 5.6±0.5 μm in PRC1 siRNA treated cells, whilst the value of the same parameter in nontargeting treated cells is 5.3±0.6 μm. This analysis, when compared to tubulin-GFP measurements performed by Kajtez and Solomatina (measured length is 11.1±1.2 μm and half-width is 5.0±0.7 μm (52 cells)), showed that spindle length and width weren't perturbed in cells with decreased expression of PRC1. In addition to these parameters, from these measurements angle at the kinetochore and angle at the centrosome were extracted by fitting a line through three points in the vicinity of the gap between kinetochores (for kinetochore angle) and through first three points of the contour (for centrosome angle). Angle at the centrosome was determined 1μm away from the centrosome and the angle at kinetochore was calculated at the end of the k-fiber, i.e. at kinetochore. These measurements were conducted in time frames following the laser ablation. Measured angle near the centrosome in PRC siRNA is 66.1±9.4 (n=26), and the angle at kinetochores in same cells is 12.5±11.8 (n=26). In this way it was possible to calculate the straightening of the cut spindle element which occurs as a consequence of the applied ablation. These values were used for calculating the amount of force acting on the centrosome and on the kinetochore. This work was done by Maja Novak in group of Nenad Pavin at Physical department of Faculty of Science in Zagreb. By introducing a physical model in study of the bridging bundle, it was possible to calculate certain values that couldn't be measured in performed experiments. By combining my experimental data with theoretical model it was possible to describe the system in more detail. By using analyzed experimental input (spindle length and width, angle at the centrosome, angle at the kinetochore, and the number of microtubules in

the bridging bundle) following parameters were calculated as the output of the physical model: position of the junction point (point of interaction between the k-fiber and the bridging bundle, which will be described in chapter “Discussion”), force at the kinetochore and force at the centrosome. The angle between the pole and sister kinetochores in the spindle element increased by 1.4±1 degrees after the cut (Figure 25).

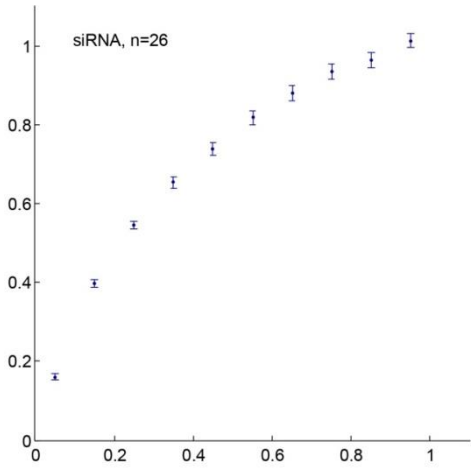


Figure 24. Average spindle contour as measured in PRC1 siRNA treated cells with error bars representing standard deviation. The plot is given as curvature that can be described along one sister k-fiber extending from the spindle pole and ending at the kinetochore. Values are normalized with centrosome position in value 0 and with position of sister kinetochore further from the ablation set to value 1.

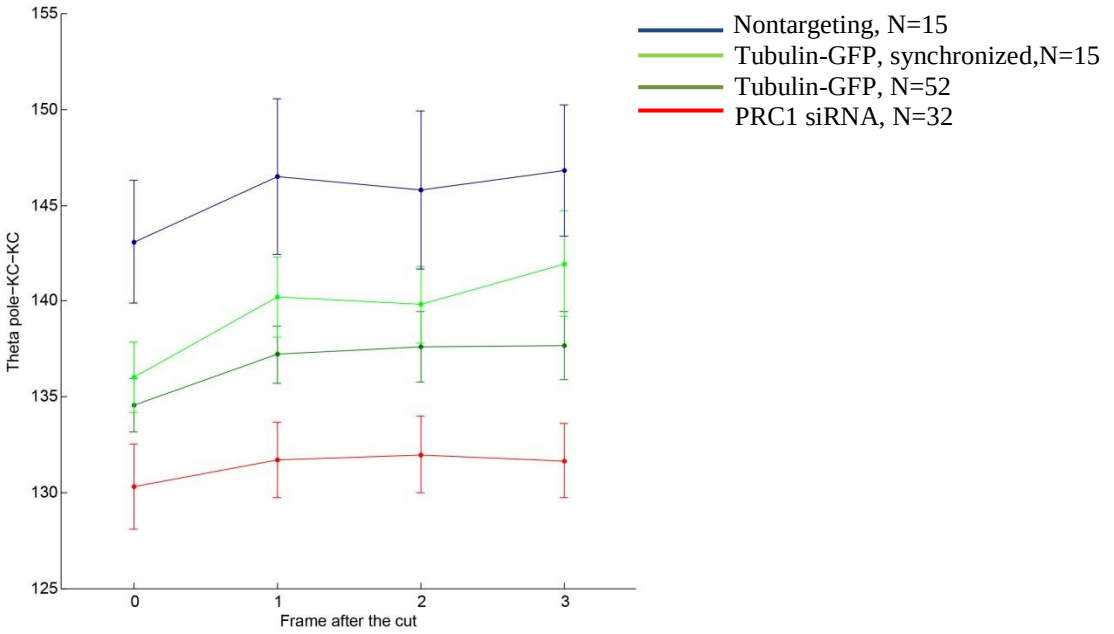


Figure 25. Straightening of the cut spindle element as a response to applied ablation. The change in angle between the spindle pole and the kinetochores ("Theta pole-KC-KC") is tracked during three time frames after the performed ablation (frame after cut). Measured value of the t-test gave p-value: p=0,321 for comparing the change in "angle pole-KC-KC" between PRC1 siRNA and tubulin-GFP. This calculation showed insignificant difference.

3.3.4. Analysis of PRC1 expression in siRNA treated cells

3.3.4.1. Immunocytochemistry

When changing the expression levels of proteins, which will teach explorer about the system he studies, it is important to quantitatively determine the level of abundance of protein of interest. There are several approaches one can choose to quantitatively describe the level of knockdown or overexpression of proteins affecting the studied system. In our experiments, a good approach would be to determine the level of knockdown in cells that were imaged and analyzed, rather than determining the abundance of chosen protein in the whole population of cells, which would be revealed by, for example, Western blot. Thus, immunocytochemistry was the preferred approach in determining the amount of PRC1 protein in analyzed cells. By labeling the dish with treated cells before experiment with laser ablation, and saving the x and y positions of individual cells, it would be possible to place the dish in the same orientation and find the exact same cells after performing the immunocytochemistry protocol. Thus, the level of protein of interest could be determined in cells that were analyzed and this data could be correlated with the laser ablation outcome. Eventually, the analysis conducted in this way would enable us to compare it between individual cells. Although the method itself wasn't reliable at the moment, the protocol has eventually been improved. The major issue was to rely on the positions that were saved in the software that controls the imaging system. If an error occurs in the x and y position values, it is impossible to find the same analyzed cells. Since the population of cells in the dish was synchronized there were many mitotic cells in the dish. Further on, the secondary response occurs in a way that the cells with applied ablation cannot be distinguished from the cells that weren’t used in the experiment at the moment. For these two reasons it was important to rely on the positions saved by the system. The protocol was improved on several levels. First, I tried out two chemicals usually used to fix cells. Methanol turned out to be better in comparison to paraformaldehyde. Whilst paraformaldehyde preserves mitotic chromosomes, methanol preserves the morphology of microtubules. Since I was interested in analyzing tubulin associated proteins, methanol was used. In addition to this improvement, I prolonged the incubation time (2 days) for the primary antibodies and got better results (Figure 26).

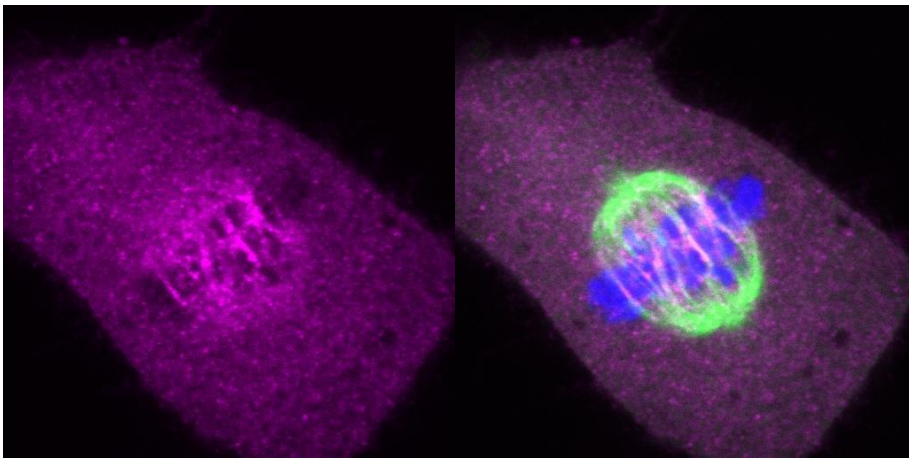


Figure 26. Improved immunocytochemistry protocol showing localization of PRC1 protein (red) in the spindle. It is expected for this protein to be most abundant in the spindle midzone. Left image corresponds to PRC1 only (Alexa fluor 555 F), whilst image on the right is acquired in the same cell with tubulin shown in green (GFP) and chromosomes in blue (DAPI). Images are acquired on Zeiss LSM 710 NLO inverted laser scanning microscope with a Zeiss PlanApo with 63x/1.4 oil immersion objective (Zeiss, Jena, Germany).

3.3.4.2. Western blot

In order to quantify the abundance of proteins in a studied system, it is possible to perform the western blot as a method that is used to detect specific proteins of interest in a sample or lysate. If compared with different control populations (control sample or lysate) it is possible to estimate the relative abundance of protein of interest in analyzed system. In that way, western blot is often used to estimate the level of knockdown or overexpression of proteins. This method is additionally useful in determining the parameters of the experiment (e.g. concentration of used chemicals) prior to collecting the statistically relevant data of perturbed system. In my experiment it was important to quantitatively describe the level of knockdown of PRC1 in order to show that my measured data (when compared to control cells) is a consequence of conducted experiment. In addition to previously described immunocytochemistry, western blot should reveal the level of PRC1 in population of RNAi treated cells. Quantification of PRC1 protein was performed in PRC1 siRNA treated cells, nontargeting control cells and in untreated HeLa cell line stably expressing tubulin-GFP

(Figure 27). Western blot was only partially successful in revealing difference in levels of PRC1 protein in treated cells and HeLa cell line stably expressing tubulin in GFP.

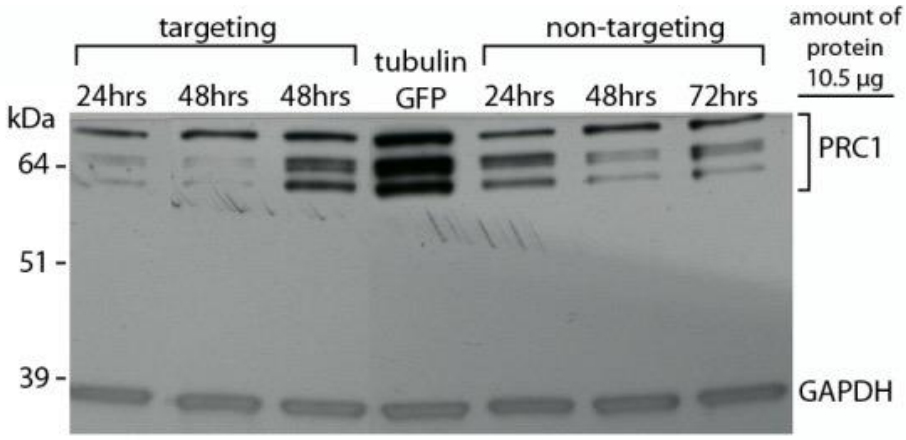


Figure 27. Western blot for PRC1 protein in siRNA treated cells (targeting), untreated HeLa cell line stably expressing tubulin in GFP (tubulin) and nontargeting treated cells (non-targeting). 24, 48 and 72 hrs represent different time points at which proteins were isolated. Western blot reveals slightly lower amount of PRC1 protein in PRC1 siRNA in comparison to nontargeting. GAPDH was used as a loading control since it is stably and constitutively expressed in most tissues and cells.

3.4. Analysis of microtubule dynamics in EB3 experiment

Other approach in understanding the bridging bundle was led by the fact that microtubule dynamics is a major property of all microtubule populations in the spindle. The idea was to analyze their growth throughout the spindle. In this experiment, HeLa cell line stably expressing 2xGFP-EB3 and mCherry-CENP-A was used. In HeLa cells with labeled end binding proteins, the spindle is seen as a rush of comets that make the contour of the whole spindle. In chosen cell line, the laser ablation was performed on the outermost k-fiber so as to achieve dissociation of a cut spindle element away from the rest of rushing comets in the spindle. I hypothesized that it would be possible to observe microtubule dynamics in the region between sister kinetochores. Depending on the response to applied ablation, cells with clear events in the cut spindle element were selected for further analysis. Since bridging fiber is composed of antiparallel microtubules, I expected to see comets passing between sister kinetochores in two directions.

Out of 338 videos with applied ablation, in 163 videos interkinetochore distance decreased after performed ablation and in 168 videos outward movement of the spindle element was achieved. Depending on the laser ablation outcome, 16 cells with maximum displacement and clear events in the region between sister kinetochores, were selected for further analysis.

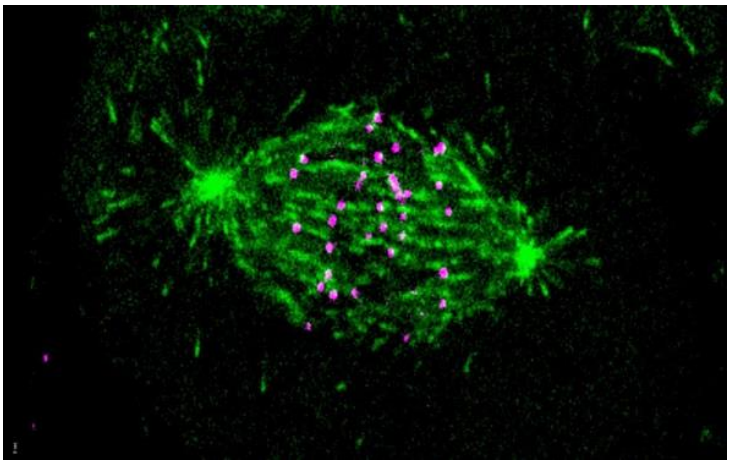


Figure 28. Mitotic spindle at the beginning of anaphase in HeLa cell line with EB3 labeled green (GFP) and kinetochores red (CENP-A-mCherry) as seen under Zeiss LSM 710 NLO inverted laser scanning microscope.

3.4.1. Determination of microtubule growth rate and microtubule dynamics in bridging bundle

EB3 cell line makes it possible to determine the growth rate of different classes of microtubules that make the spindle. Velocity of their growth was measured in ImageJ as described in chapter "Materials and methods", section "Image analysis in EB3 experiment".
Measured velocity of individual growing astral microtubules was 0.2±0.04 μm/s, (69 comets). Microtubules in the k-fiber grow with measured velocity of 0.22±0.02 μm/s, (12 comets). Finally, microtubules in the region between sister kinetochores grow with measured velocity of 0.22±0.02 μm/s, (16 comets).
In the cut spindle element it was possible to distinguish comets that either stopped at first sister kinetochore they met or, alternatively, passed between sister kinetochores. The comets that passed between sister kinetochores were counted only when it was possible to observe them exclusively in the region between sister kinetochores. For this reason laser ablation was used to achieve the dissociation of the cut spindle element away from the rest of the spindle (Figure 29). Number of comets that stop and pass was determined either by eye, making montage of the selected time or finally by visualizing microtubule dynamics during selected time by using kymograph (Figure 30). Release of compression and tension were not analyzed in this experiment.

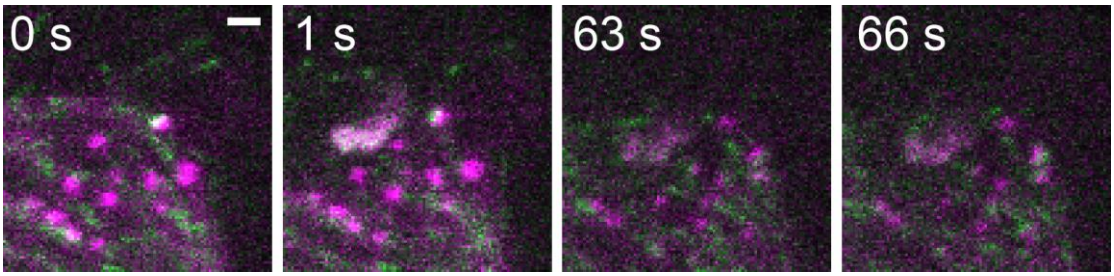


Figure 29. Laser ablation response in HeLa cell line stably expressing EB3-GFP (Green) and mCherry-CENP-A (magenta). At 63rd second (s) and 66th second after ablation a comet is seen passing between sister kinetochores. White bar represents 1 μm scale bar.

a)

b)

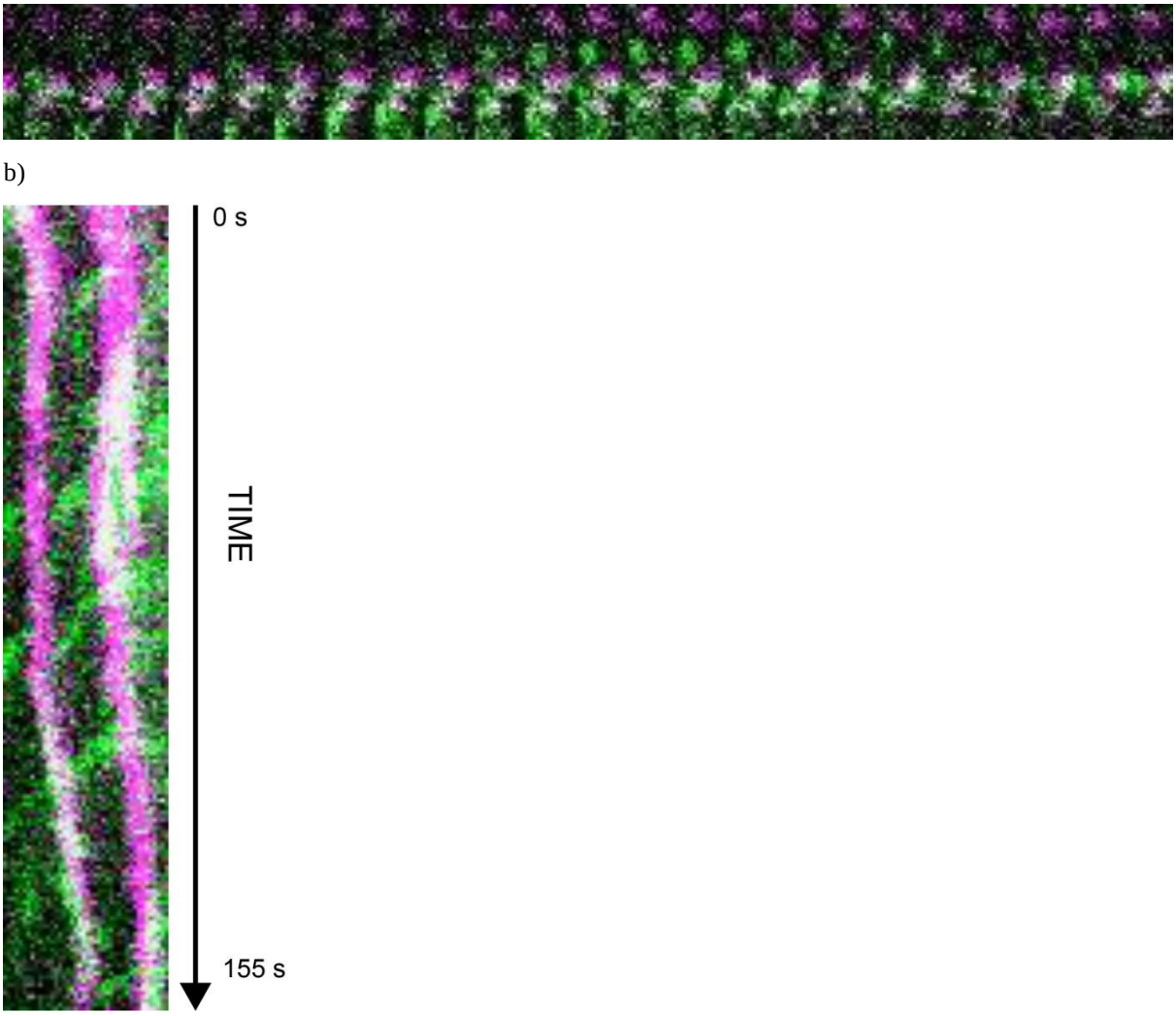


Figure 30. a) Selected part of montage of the video from above with comet passing between sister kinetochores. b) Kymograph of the entire selected time with clear events in the region between sister kinetochores. Note that in the kymograph 5 comets pass between, so one EB3 comet in the montage corresponds to one comet in the kymograph.

Comets that stop at first sister kinetochore they meet are interpreted as microtubules that grow in the k-fiber, and I detected 2.78±0.12 comets per minute. Comets that pass between sister kinetochores are interpreted as microtubules that grow in the bridging microtubule fiber, and I detected 2.42±0.1 comets per minute. If measured by eye, 2.42±0.1 comets pass between sister kinetochores, whilst kymograph revealed 2.6±1 passing between.

In one cut spindle element, comets that pass between sister kinetochores, both from the ablation site, 0.57±0.05 comets per minute, as well as from the connection, 1.85±0.1 comets per minute were observed. This additionally confirms that bridging microtubule bundle is composed of antiparallel microtubules. All error values are given as standard deviation.

4. DISCUSSION

4.1. Force balance in the mitotic spindle

Mitotic spindle is a truly remarkable assembly that orchestrates equal distribution of chromosomes to two daughter cells. Errors in its performance often lead to chromosome missegregation which can have serious consequences, like birth defects and can lead to cancerous cells. In the past decades a lot has been revealed about its composition, mechanics and performance. Described microtubules, kinetochores and motor and non-motor proteins direct the spindle's behavior. However, our understanding is still far from complete. It is not completely clear how all the components intermingle within and around the spindle and how they mutually direct each other's behavior. What is clear is that it is all about the forces acting within the spindle. They are dependent on biophysical properties of molecules that intermingle throughout the spindle. Molecular motors, microtubule dynamic instability, elastic elements and friction are lead actors in force generation [51]. These forces drive chromosome capture, their biorientation and oscillations, their alignment in the metaphase plate and eventually synchronous separation and equal distribution to new daughter cells.

Force map in the spindle has already been analyzed and it is known that there is compressive and tensile force acting within one spindle element. One cannot help but ask how these opposing forces act along a single spindle element which can be imagined as elastic rod. The compression could have its origin in the fact that astrals, which interact with the cell cortex, polymerize on the cell boundaries and thus could exert force on the spindle poles [74]. However, in some cases spindle moved a lot within the cell, whilst preserving its shape. Could the motor proteins acting between the astrals and the cortex contribute to its rapid movement inside the cell? On the other hand, compressive force could originate from within the spindle itself. Since a term spindle matrix comprises all motor and nonmotor proteins acting in the spindle, all of them together could contribute to certain inward forces. Motor proteins as dynein and some minus end directed kinesins could increase the span of antiparallel regions [75], which could further become more stable by recruitment of nonmotor crosslinking proteins. At the same time, mechanical tension between sister kinetochores signals proper biorientation of chromosomes on microtubules of the mitotic spindle and selectively stabilizes these attachments [76]. The stabilization of tensile force and kinetochore attachment to microtubule is highly regulated by Aurora B kinase, which phosphorylates key

microtubule-binding elements within the kinetochore [77]. We were interested in analyzing how these opposing forces are distributed along one spindle element. Many have wondered about the forces in the spindle, and there was a need to introduce some unidentified compensating components: "How is tension generated on k-fibers, and how is it balanced by compression in other spindle components?" [51]. "Primitive" force maps of the spindle suggested that non-kinetochore microtubules bear the compressive load that would balance tension at kinetochores [51]. Whilst some discussed the spindle matrix and its components (NuMa, Skeletor, poly(ADP-ribose)), others were quite clear about the requirements for some yet unidentified element that would balance compressive force near poles and tensile force at kinetochore (Figure 31), [51]. Further on, as already mentioned, antiparallel microtubules do not exclusively have their minus ends fixed at poles, but are rather localized throughout the spindle. It was stated that many non-kinetochore microtubules have their minus ends embedded in k-fibers, where they presumably couple mechanically to kinetochore microtubules [55]. We believe that it is the bridging bundle that could balance these opposing forces by linking sister k-fibers, thus regulating the transition from compression to tension along one spindle element. In experiments conducted here and elsewhere [50; 69], it was shown that as a response to applied ablation, both compressive and tensile force are released in the cut part of the spindle. What makes sense in understanding the force distribution, is to perturb it. Since we believe that the bridging bundle is a good candidate, it seemed that by changing it, we could analyze the difference in response to the ablation. By reducing its thickness we expected to achieve less compression, and by applying laser ablation, it would be possible to describe some difference. What couldn't be expected is the greatness of effect on the spindle as well as on the laser ablation outcome. Even though the difference in primary response is not very different from our control, the system was slightly perturbed. Successful experiments were recently performed with the same logic, but with opposite approach. In experiments in which the bridging bundle was made thicker, the different primary response was obvious in comparison to control cells. In these particular experiments, antiparallel bundles were made thicker by overexpressing crosslinking protein PRC1 and tubulin [50; 69]. The laser ablation outcome in their experiments was shown to be more pronounced in comparison to untreated cells. In particular, outward movement, as the primary response to ablation, was faster. As the bridging bundle is composed of antiparallel microtubules, their thickness was also increased, thus indicating that the amount of compressive force acting in the spindle element was increased. By reducing levels of the same protein, we managed to slightly reduce the bridging microtubule thickness. But how does the reduced level of

crosslinking protein produce decreased antiparallel bundle thickness? Does the absence of one protein in that region just make more space for other proteins to get recruited to their localization spot? Further on, what is the lowest possible velocity of the outward movement? If it is possible to achieve no outward movement as a response to applied ablation, it would mean that there is no compressive force in the spindle. In this case, would it be possible for spindle to assemble at all and to perform its function of segregating chromosomes? Regardless of questions that remain to be answered, we believe that bridging bundle contributes to the force map in the spindle and results of performed experiments show that it could be the best candidate for performing this role.

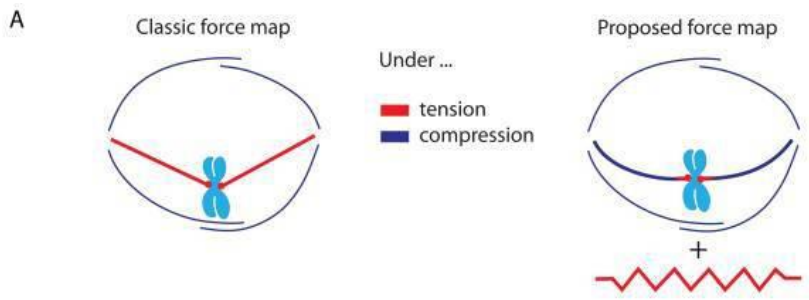


Figure 31. Scheme of a proposed force map in the spindle with compression and tension acting "back to back" within individual spindle components, i.e. k-fibers [51].

Considering the fact that the bridging bundle, being composed of antiparallel microtubules, stores certain motor and non-motor proteins within, basic forces these proteins exert are acting as well within bridging bundle. The activity of plus-end directed motors between antiparallel microtubules drives their sliding, known as the poleward flux. It is known that the poleward flux acts in k-fibers, but since individual k-fibers have uniform polarity, it is not clear how this would be achieved. Now that it is clear that a novel structural component is present in the spindle, many unclear activities could be unraveled. Since they are a lateral connection between two sister k-fibers, and contain microtubules of opposite polarity comprised within, it is quite possible that it is the bridging bundle that drives this activity. Since this mechanism, driven by motor proteins, is involved in anaphase, this would mean

that the bridging bundle could contribute to this phase of the cycle. In experiments including laser ablation at precise time right before anaphase, one would expect to see the interkinetochore distance decrease (release of tension) and immediate continuous increase in interkinetochore distance that indicates the beginning and continuation of anaphase. Indeed, it was shown already that chromosomes can get segregated without one of the sister k-fibers being connected to one pole [78]. In those experiments, evidence was presented for dynein to mediate the poleward movement that segregates chromosomes that lack the connection to one pole. In other proposed mechanism, called the Pacman activity, chromosomes are segregated due to depolymerizing k-fiber microtubules at the kinetochore [79; 80; 81]. It is thought that, when the tension between kinetochores is lost as the response to applied ablation, the Pacman mechanism gets activated [81]. Regardless of these findings, we speculate that it is the poleward flux acting within antiparallel microtubules in the bridging bundle that drives these events.

4.2. Junction point

Since bridging bundle is a mechanical connection between sister k-fibers, there has to be some sort of junction point of bridging bundle on each sister k-fiber. This point of interaction could be imagined as a merging or a branching point. Indeed certain experiments already indicate that there is a strong possibility for their existence [69]. In experiments designed with the position of the cut with respect to the junction point, it was shown that interkinetochore distance sometimes doesn't change. It was proposed that when the cut is positioned between junction point and kinetochore, the interkinetochore distance was reduced since the connection between k-fiber and the bridging bundle is partially lost. In that case tension would be released and interkinetochore distance would be reduced. On the other hand, if the cut is positioned in a way that junction point becomes part of the cut element that moves outwards, tension would be preserved and interkinetochore wouldn’t change. Since there are firm indications for the presence of junction point, it would become a novel component in the composition of the spindle as well as the bridging bundle itself. It would be interesting to see wether it could be the boarder point of kinetochore oscillations. Chromosome oscillations, which eventually position them in the metaphase plate are driven by summing of stochastic

forces at the kinetochore and chromosome arms along with dynamic instability of microtubules [82]. If microtubule depolymerases could act beyond junction point in direction towards the spindle pole, what would happen with that point of interaction between the bridging bundle and the k-fiber? If depolymerases would "consume" the junction point, that would probably mean that the bridging bundle would undergo loss of interaction with the k-fiber. Thus, one could more easily imagine that the junction point itself could oscillate on the k-fiber. These oscillations could, at certain time points, be independent of the chromosome oscillations but often they could be driven by the chromosome oscillations as well (Figure 32).

Although experiments performed in this thesis did not question the precise biological function of bridging microtubule bundle, one cannot help but wonder about its possible roles throughout mitosis.

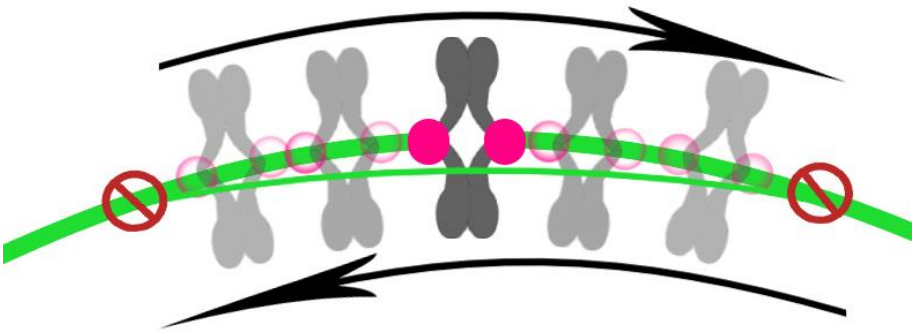


Figure 32. Scheme of postulated chromosome oscillations coupled with the bridging bundle region.

4.3. Secondary response

Secondary response to the laser microsurgery is the reconnection of the ablated spindle element back to the spindle. Since in experiments conducted here it is observed in majority of analyzed cells, it is not a coincidence. This behavior was already shown and analyzed in other research groups. It was shown that dynein pulls the stub back towards spindle's center of mass and helps it reintegrate in the spindle. After the cut, some time is needed for dynein to accumulate on the newly formed minus end of the stub. At one point, the stub would be reconnected to some adjacent microtubules and get pulled towards one of the spindle poles

[48]. Laser microsurgery is not something that would happen normally in the spindle, but still it is able to recover from such a perturbation. Since it is fundamental for chromosomes to get equally and synchronously segregated, there are many self-repair mechanisms that correct different types of errors in the spindle structure and performance. Reconnection results in reestablishment of forces that were released after microsurgery. If the reconnection occurs in a normal way, the forces are reestablished and regular subsequent events can unravel. Chromosomes in the cut spindle element can begin oscillating again and further steps of the process, e.g. anaphase, can be carried out.

4.4. Dynamics of bridging microtubules

We have shown in HeLa cell line stably expressing 2xGFP-EB3 that there is a certain microtubule dynamics present in a region between sister kinetochores. The conclusion is that it is occurring within the bridging microtubule bundle. By using laser ablation, we managed to observe clear events of microtubule growth both in direction from intact k-fiber, as well as from direction of ablation site, thus confirming the antiparallel composition of bridging fiber. These experiments were performed in order to see whether some microtubules grow beyond first sister kinetochore they encounter. Since it was believed that k-fiber is capped on the kinetochore, some growing microtubules between sister kinetochores would reveal a bundle located in between. Since in most observed cases comets were observed clearly growing from one sister kinetochore towards other sister kinetochore, one wouldn’t think that they are just simply astral microtubules growing in a random way. In these experiments it was difficult to quantify where the starting point of their growth is so we didn’t focus on that particular analysis. Within the selected time, we observed comets stopping at first kinetochore, thus revealing growing microtubules in the k-fiber. Comets showing growing microtubules in the k-fiber would typically pile up on kinetochore and some would eventually continue growing towards the other sister kinetochore. This observation suggests that the bridging microtubules grow in direct proximity of the k-fibers and branch out to form the bridging bundle. How is their growth directed in a way that they eventually meet the following sister k-fiber if there already aren’t any microtubules present?

Quantification of dynamics in k-fiber and bridging fiber revealed the similar growth rate in both. The role of the bridging microtubules was not investigated in EB3 experiment. Our hypothesis was that, if there are some microtubules laterally connecting the sister k-fibers, we should be able to observe growing microtubules in the region between sister kinetochores which was experimentally confirmed. Measurements of microtubule growth rate are consistent with previously measured data [83]. By measuring the growth rate of microtubules in the bridging fiber, it is shown that they grow with same velocity as the ones in the k-fiber. This suggests that their growth is regulated in a similar manner as the growth of other populations of microtubules in the spindle, thus revealing the same nature of bridging microtubules as of those that are already known.

5. Conclusions

From the text books, k-fibers stop when they bind to kinetochores and it was assumed that sister k-fibers are not in direct contact. In this project we recognized that there is a bundle of non-kinetochore antiparallel microtubule bundle spanning the region between sister kinetochores and it was named bridging microtubule bundle. From two different point of views the analysis of this bundle was conducted.

In one experiment my goal was to test whether some microtubule dynamics could be observed in the region between sister kinetochores. To test this, the laser ablation assay was applied. It helped me to distinguish certain events in the chosen region of the spindle. This experiment was performed in a cell line stably expressing end binding protein and a kinetochore protein. After collecting cells with good signal by performed FACS (fluorescence activated cell sorting), this experiment was significantly improved. Laser microsurgery made it possible for me to describe certain clear events and I observed microtubules growing in opposite directions in the region between sister kinetochores and they were interpreted as those growing in the bridging microtubule bundle.

The other experiment was performed in order to perturb the role of bridging fiber in the distribution of forces in the spindle. I believed that this could be achieved by reducing the level of protein that crosslinks antiparallel microtubules in the bridging fiber. Laser ablation was performed here as well, since it teaches us about the forces acting in the cut spindle element. I expected the outward movement to be less pronounced and to have lower velocity in comparison to control cells. I suspect that the chemicals used in synchronization protocol affected the conditions in treated cells. In order to minimize the treatment of cells, I would prefer not to synchronize them in further experiments. Even though conducted analysis did not reveal significant difference between control cells and PRC1 siRNA treated cells, this experiment indicates the right approach to perturbing the force balance, which will be further investigated.

6. References

1. Pawley JB: Handbook of Biological Confocal Microscopy (3rd ed.), Springer, 2006
2. Hook R: Micrographia, The Royal Society, London, 1665
3. Paweletz N, Walther Flemming: pioneer of mitosis research. Nat Rev Mol Cell Biol, 2(1): 72-75, 2001
4. http://spirochrome.com/gallery/
5. Scherer WF, Syverton JT, Gey GO: Studies on the propagation in vitro of poliomyelitis viruses. IV. Viral multiplication in a stable strain of human malignant epithelial cells (strain HeLa) derived from an epidermoid carcinoma of the cervix, J Exp Med, 97(5): 695–710, 1953
6. http://users.minet.uni-jena.de/csb/prj/cellcycle/
7. Alberts B, Johnson A, Lewis J, Raff M, Roberts K, Walter P: Molecular biology of the cell, Garland Science, Taylor & Francis Group, 2002
8. McIntosh JR, Molodtsov MI, Ataullakhanov FI: Biophysics of mitosis, Q Rev Biophys, 45(2): 147-207, 2012
9. Hartwell LH, Culotti J, Reid B: Genetic control of the cell-division cycle in yeast. I. Detection of mutants, Proc Natl Acad Sci U S A, 66(2): 352-359, 1970
10. Murray A: Cell cycle checkpoints, Curr Opin Biol, 6(6): 872-876, 1994
11. http://oregonstate.edu/instruction/bi314/fall11/cellcycle.html
12. Nigg EA, Stearns T: The centrosome cycle: centriole biogenesis, duplication and inherent asymmetries, 13(10): 1154-1160, 2011
13. Wiese C, Zheng Y: Microtubule nucleation: gamma-tubulin and beyond, Journal of Cell Science, 119(20): 4143-4153, 2006
14. http://www.mueller-reichert-lab.de/research.html

15. https://molgen.osu.edu/people/fisk.13

16. Mitchison T, Kirschner ML: Dynamic instability of microtubule growth, Nature, 312(5991): 237-242, 1984

17. Walker RA, O'Brien ET, Pryer NK, Soboeiro MF, Voter WA, Erickson, HP, Salmon, ED: Dynamic instability of individual microtubules analyzed by video light microscopy: rate constants and transition frequences, J Cell Biol, 107(4): 1437-1448, 1988

18. Brouhard GJ: Dynamic instability 30 years later: complexities in microtubule growth and catastrophe, Mol Biol Cell, 26(7): 1207-1210, 2015

19. Salmon ED, Leslie RJ, Saxton WM, Karow ML, McIntosh JR: Spindle microtubule dynamics in sea urchin embryos: analysis using a fluorescein-labeled tubulin and
measurements of fluorescence redistribution after laser photobleaching, J Cell Biol, 99(6): 2165-2174, 1984

20. Inoue S: Polarization optical studies of the mitotic spindle. I. The demonstration of spindle fibers in living cells, Chromosoma, 5(5): 487-500, 1953

21. Conde C, Cáceres A: Microtubule assembly, organization and dynamics in axons and dendrites Nat Rev Neurosci, 10(5): 319-332, 2009

22. Brinkley BR, Stubblefield E: The fine structure of the kinetochore of a mammalian cell in vitro, Chromosoma, 19(1): 28-43, 1966

23. Telzer BR, Moses MJ, Rosenbaum JL: Assembly of microtubules onto kinetochores of isolated mitotic chromosomes of HeLa cells, Proc Natl Acad Sci U S A, 72(10): 4023-7, 1975

24. Witt PL, Ris H, Borisy GG, Origin of kinetochore microtubules in Chinese hamster ovary cells, Chromosoma, 81(3): 483-505, 1980

25. De Brabander M, Geuens G, De Mey J, Joniau M: Nucleated assembly of mitotic microtubules in living PTK2 cells after release from nocodazole treatment, Cell Motil, 1(4): 469–483, 1981

26. Tulu US, Fagerstrom C, Ferenz NP, Wadsworth P: Molecular requirements for kinetochore-associated microtubule formation in mammalian cells, Curr Biol, 16(5): 536–541, 2006

27. Maiato H, Rieder CL, Khodjakov A: Kinetochore-driven formation of kinetochore fibers contributes to spindle assembly during animal mitosis, J Cell Biol, 167(5): 831–840, 2004

28. Pavin N, Tolić-Nørrelykke IM: Swinging a sword: how microtubules search for their targets, Syst Synth Biol, 8(3): 179-186, 2014

29. Lodish H, Berk A, Zipursky SL, Matsudaira P, Baltimore D, Darnell J: Molecular cell biology, W. H. Freeman, 2000

30. https://www.sciencenews.org/article/view-cell

31. Manning AL, Compton DA: Structural and regulatory roles of nonmotor spindle proteins, Curr Opin Cell Biol, 20(1): 101-106, 2008

32. Merdes A, Heald R, Samejima K, Earnshaw WC, Cleveland DW: Formation of spindle poles by dynein/dynactin-dependent transport of NuMA, J Cell Biol, 149(4): 851-862, 2000

33. Zhu C, Lau E, Schwarzenbacher R, Bossy-Wetzel E, Jiang W: Spatiotemporal control of spindle midzone formation by PRC1 in human cells, Proc Natl Acad Sci U S A, 103(16): 6196-6201, 2006

34. Tirnauer JS, Bierer BE: EB1 proteins regulate microtubule dynamics, cell polarity, and chromosome stability, J Cell Biol, 149(4): 761-766, 2000

35. Komarova Y, De Groot CO, Grigoriev I, Gouveia SM, Munteanu EL, Schober JM, Honnappa S, Buey RM, Hoogenraad CC, Dogterom M, Borisy GG, Steinmetz MO, Akhmanova A: Mammalian end binding proteins control persistent microtubule growth, J Cell Biol, 184(5): 691-706, 2009

36. Akhmanova A, Steinmetz MO: Tracking the ends: a dynamic protein network controls the fate of microtubule tips, Nat Rev Mol Cell Biol, 9(4): 309-322, 2008

37. Sandblad L, Busch KE, Tittmann P, Gross H, Brunner D, Hoenger A: The Schizosaccharomyces pombe EB1 homolog Mal3p binds and stabilizes the microtubule lattice seam, Cell, 127(7): 1415-1424, 2006

38. des Georges A, Katsuki M, Drummond DR, Osei M, Cross RA, Amos LA: Mal3, the Schizosaccharomyces pombe homolog of EB1, changes the microtubule lattice, Nat Struct Mol Biol, 15(10): 1102-1108, 2008

39. Vitre B, Coquelle FM, Heichette C, Garnier C, Chrétien D, Arnal I: EB1 regulates microtubule dynamics and tubulin sheet closure in vitro, Nat Cell Biol, 10(4): 415-421, 2008

40. Mimori-Kiyosue Y, Shiina N, Tsukita S: The dynamic behavior of the APC-binding protein EB1 on the distal ends of microtubules, Curr Biol, 10(14): 865-868

41. Berrueta L, Kraeft SK, Tirnauer JS, Schuyler SC, Chen LB, Hill DE, Pellman D, Bierer BE: The adenomatous polyposis coli-binding protein EB1 is associated with cytoplasmic and spindle microtubules, Proc Natl Acad Sci U S A, 95(18): 10596-10601, 1998

42. Morrison EE, Askham JM: EB 1 immunofluorescence reveals an increase in growing astral microtubule length and number during anaphase in NRK-52E cells, Eur J Cell Biol, 80(12): 749-753, 2001

43. Piehl M, Tulu US, Wadsworth P, Cassimeris L: Centrosome maturation: measurement of microtubule nucleation throughout the cell cycle by using GFP-tagged EB1, Proc Natl Acad Sci U S A, 101(6): 1584-1588, 2004

44. Pavin N, Tolić-Nørrelykke IM: Dynein, microtubule and cargo: a ménage à trois, Biochem Soc Trans, 41(6): 1731-1735, 2013

45. Vogelsberg CS, Garcia-Garibay MA: Crystalline molecular machines: function, phase order, dimensionality, and composition, Chem Soc Rev, 41(5): 1892-1910, 2012

46. Wordeman L: How kinesin motor proteins drive mitotic spindle function: Lessons from molecular assays, Semin Cell Dev Biol, 21(3): 260-268, 2010

47. Elting MW, Hueschen CL, Udy DB, Dumont S: Force on spindle microtubule minus ends moves chromosomes, J Cell Biol, 206(2): 245-256, 2014

48. Civelekoglu-Scholey G, Scholey JM: Mitotic force generators and chromosome segregation, Cell Mol Life Sci, 67(13): 2231-2250, 2010

49. Walczak CE, Cai S, Khodjakov A: Mechanisms of chromosome behaviour during mitosis, Nat Rev Mol Cell Biol, 11(2): 91-102, 2010

50. Solomatina A: Force balance in the mitotic spindle of HeLa cells studied by high-speed live-cell imaging, Technische Universität Dresden, 2014

51. Dumont S, Mitchison TJ: Force and length in the mitotic spindle, Curr Biol, 19(17): 749-761, 2009

52. Mitchison TJ, Maddox P, Gaetz J, Groen A, Shirasu M, Desai A, Salmon ED, Kapoor TM: Roles of polymerization dynamics, opposed motors, and a tensile element in governing the length of Xenopusextract meiotic spindles, Mol Biol Cell, 16(6): 3064-3076, 2005.

53. Wühr M, Chen Y, Dumont S, Groen AC, Needleman DJ, Salic A, Mitchison TJ: Evidence for an upper limit to mitotic spindle length, Curr Biol, 18(16): 1256-1261, 2008.

54. Mastronarde DN, McDonald KL, Ding R, McIntosh JR: Interpolar microtubules in PTK cells, J Cell Biol, 123(6 Pt 1), 1475-1489, 1993

55. Burbank KS, Groen AC, Perlman ZE, Fisher DS, Mitchison TJ: A new method reveals microtubule minus ends throughout the meiotic spindle, J Cell Biol, 175(3): 369-75, 2006.

56. Gatlin JC, Bloom K: Microtubule motors in eukaryotic spindle assembly and maintenance, Semin Cell Dev Biol, 21(3): 248-254, 2010

57. Rusan NM, Fagerstrom CJ, Yvon AM, Wadsworth P: Cell cycle-dependent changes in microtubule dynamics in living cells expressing green fluorescent protein-alphatubulin, Mol Biol Cell, 12(4): 971-80, 2001

58. Waterman-Storer CM, Desai A, Bulinski JC, Salmon ED: Fluorescent speckle microscopy, a method to visualize the dynamics of protein assemblies in living cells, Curr Biol, 8(22): 1227-1230, 1998

59. Verde F, Berrez JM, Antony C, Karsenti E: Taxol-induced microtubule asters in mitotic extracts of Xenopus eggs: requirement for phosphorylated factors and cytoplasmic dynein, J Cell Biol, 112(6): 1177-1187, 1991

60. Gaglio T, Saredi A, Compton DA: NuMA is required for the organization of microtubules into aster-like mitotic arrays, J Cell Biol, 131(3): 693-708, 1995

61. Tanaka TU, Stark MJ, Tanaka K: Kinetochore capture and bi-orientation on the mitotic spindle, Nat Rev Mol Cell Biol, 6(12): 929-42, 2005

62. Kalab P, Pu RT, Dasso M: The ran GTPase regulates mitotic spindle assembly, Curr Biol, 9(9): 481-484, 1999

63. Sampath SC, Ohi R, Leismann O, Salic A, Pozniakovski A, Funabiki H: The chromosomal passenger complex is required for chromatin-induced microtubule stabilization and spindle assembly, Cell, 118(2): 187-202, 2004

64. Carmena M, Wheelock M, Funabiki H, Earnshaw WC: The chromosomal passenger complex (CPC): from easy rider to the godfather of mitosis, Nat Rev Mol Cell Biol, 13(12): 789-803, 2012

65. Pfarr CM, Coue M, Grissom PM, Hays TS, Porter ME, McIntosh JR: Cytoplasmic dynein is localized to kinetochores during mitosis, Nature, 345(6272): 263-265, 1990

66. Kim Y, Heuser JE, Waterman CM, Cleveland DW: CENPE combines a slow, processive motor and a flexible coiled coil to produce an essential motile kinetochore tether, J Cell Biol, 181(3): 411–419, 2008

67. Wordeman L, Wagenbach M, von Dassow G: MCAK facilitates chromosome movement by promoting kinetochore microtubule turnover, J Cell Biol, 179(5): 869-879, 2007

68. http://imgbuddy.com/cell-division-anaphase.asp

69. Kajtez J: Study of forces in HeLa cell metaphase mitotic spindle using laser ablation, Technische Universität Dresden, 2014

70. Krull A, Steinborn A, Ananthanarayanan V, Ramunno-Johnson D, Petersohn U, Tolić-Nørrelykke IM: A divide and conquer strategy for the maximum likelihood localization of low intensity objects, Opt Express, 22(1): 210-28, 2014

71. Zhou J, Yao J, Joshi HC: Attachment and tension in the spindle assembly checkpoint, J Cell Sci, 115(Pt 18): 3547-55, 2002

72. Khodjakov A, Pines J: Centromere tension: a divisive issue, Nat Cell Biol, 12(10): 919-23, 2010

73. McEwen, BF, Heagle, AB, Cassels, GO, Buttle KF, Rieder CL: Kinetochore fiber maturation in PtK1 cells and its implications for the mechanisms of chromosome congression and anaphase onset, J Cell Biol, 137(7): 1567-1580, 1997

74. Grill SW, Hyman AA: Spindle positioning by cortical pulling forces, Dev Cell, 8(4): 461-465, 2014

75. Sharp DJ, Rogers GC, Scholey JM: Microtubule motors in mitosis, Nature, 407(6800): 41-47, 2000

76. Sarangapani KK, Asbury CL: Catch and release: How do kinetochores hook the right microtubules during mitosis?, Trends Genet, 30(4): 150-159, 2014

77. Cheeseman IM, Anderson S, Jwa M, Green EM, Kang Js, Yates JR 3rd, Chan CS, Drubin DG, Barnes G: Phospho-regulation of kinetochore-microtubule attachments by the Aurora kinase Ipl1p, Cell, 111(2):163-172, 2002

78. Sikirzhytski V, Magidson V, Steinman JB, He J, Le Berre M, Tikhonenko I, Ault JG, McEwen BF, Chen JK, Sui H, Piel M, Kapoor TM, Khodjakov A: Direct kinetochore-spindle pole connections are not required for chromosome segregation, J Cell Biol, 206(2): 231-243, 2014

79. Gorbsky GJ, Sammak PJ, Borisy GG: Chromosomes move poleward in anaphase along stationary microtubules that coordinately disassemble from their kinetochore ends, J Cell Biol, 104(1): 9-18, 1987

80. Desai A, Maddox PS, Mitchison TJ, Salmon ED: Anaphase A chromosome movement and poleward spindle microtubule flux occur at similar rates in Xenopus extract spindles, J Cell Biol, 141(3): 703-713, 1998

81. LaFountain JR Jr, Cohan CS, Oldenbourg R: Pac-man motility of kinetochores unleashed by laser microsurgery, Mol Biol Cell, 23(16): 3133-3142, 2012

82. Jaqaman K, King EK, Amaro AC, Winter JR, Dorn JF, Elliott HL, Mchedlishvili N, McClelland SE, Porter IM, Posch M, Toso A, Danuser G, McAinsh AD, Meraldi P, Swedlow JR: Kinetochore alignment within the metaphase plate is regulated by centromere stiffness and microtubule depolymerases, J Cell Biol, 188(5): 665–679, 2010

83. Sironi L, Solon J, Conrad C, Mayer TU, Brunner D, Ellenberg J: Automatic quantification of microtubule dynamics enables RNAi-screening of new mitotic spindle regulators, Cytoskeleton, 68(5): 266-278, 2011

7. BIBLIOGRAPHY

Bruno Polak

Personal information:

Date of birth: August 1, 1986.

City of birth: Zagreb, Hrvatska

Education:

Faculty of Science, Department of Biology, Graduate programme for molecular biology, 2005-today
„Prva privatna gimnazija“ Zagreb, Croatia, 2001 – 2005

Foreign languages: Croatian (mother tongue)
English (advanced level in speaking and writing)
German (middle level in speaking and writing)
Italian (middle level in speaking and writing)
Spanish (middle level in speaking and writing)

Driving license: B category